



# Deletion of wheat alpha-gliadins from chromosome 6D improves gluten strength and reduces immunodominant celiac disease epitopes

Maria G. Rottersman<sup>1</sup> · Wenjun Zhang<sup>1</sup> · Junli Zhang<sup>1</sup> · Gabriela Grigorean<sup>2</sup> · German Burguener<sup>1,3</sup> · Claudia Carter<sup>4</sup> · Teng Vang<sup>4</sup> · Joshua Hegarty<sup>1</sup> · Xiaoqin Zhang<sup>1</sup> · Sean Finnie<sup>5</sup> · Jorge Dubcovsky<sup>1,3</sup> 

Received: 9 November 2024 / Accepted: 11 March 2025 / Published online: 8 April 2025  
© The Author(s) 2025

## Abstract

Wheat gliadins and glutenins confer valuable end-use characteristics but include amino acid sequences (epitopes) that can elicit celiac disease (CeD) in genetically predisposed individuals. The onset of CeD in these individuals is affected by the amount and duration of the exposure to immunogenic epitopes. Therefore, a reduction of epitopes that result in high immune responses in the majority of CeD patients (immunodominant epitopes) may reduce the incidence of CeD at a population level. We generated gamma radiation-induced deletions encompassing the  $\alpha$ -gliadins in each of the three wheat genomes and characterized them using exome capture. These deletions, designated as  $\Delta$ gli-A2,  $\Delta$ gli-B2, and  $\Delta$ gli-D2, were deposited in GRIN-Global. The  $\Delta$ gli-A2 and  $\Delta$ gli-B2 deletions showed limited effects on breadmaking quality, but the  $\Delta$ gli-D2 deletion significantly increased gluten strength and improved breadmaking quality without compromising dough elasticity, protein content, or grain yield. The stronger effect of  $\Delta$ gli-D2 on gluten strength was associated with an increased proportion of glutenins and the deletion of  $\alpha$ -gliadins with seven cysteines, which are absent in the *GLI*-A2 and *GLI*-B2 loci. We show that  $\alpha$ -gliadins with seven cysteines are incorporated into the gluten polymer, where they likely function as chain terminators limiting the expansion of the gluten polymer and reducing its strength. In addition to its beneficial effects on breadmaking quality, the  $\Delta$ gli-D2 deletion eliminates major wheat immunodominant CeD epitopes. The deployment of this publicly available  $\Delta$ gli-D2 deletion can simultaneously improve wheat gluten strength and reduce the population-wide burden of CeD.

## Introduction

Celiac disease (CeD), a common immune-mediated condition characterized by inflammation of the small intestine, affects approximately 1% of the world's population (Bradauskienė et al. 2023), and its incidence has been increasing over time (King et al. 2020). CeD is triggered in genetically predisposed individuals by consumption of wheat gluten and gluten-like peptides. Currently, the only effective treatment for CeD is a completely gluten-free diet. However, even those who strictly adhere to a gluten-free diet may suffer from compromised health due to nutritional imbalance and a less robust gut microbiome, social isolation, and an increased cost of living (Sánchez et al. 2023).

Gluten is a protein polymer that confers viscoelastic and extensible properties to wheat bread and pasta dough. This complex includes two classes of proteins: glutenins, which are interconnected to each other by disulfide bonds at cysteine residues (CYS) to form a mesh-like structure, and gliadins, which typically form non-covalent bonds with glutenins (Shewry and Lafiandra 2022). Most glutenin and

---

Communicated by Diane E. Mather.

---

Maria G. Rottersman and Wenjun Zhang have contributed equally to this work.

 Jorge Dubcovsky  
jdubcovsky@ucdavis.edu

<sup>1</sup> Department of Plant Sciences, University of California, One Shields Avenue, Davis, CA 95616, USA

<sup>2</sup> Proteomics Core Facility, University of California, 451 E. Health Sciences Dr., Davis, CA 95616, USA

<sup>3</sup> Howard Hughes Medical Institute, 4000 Jones Bridge Rd, Chevy Chase, MD 20815, USA

<sup>4</sup> California Wheat Commission, 1240 Commerce Ave., Woodland, CA 95776, USA

<sup>5</sup> USDA-ARS E-202 Food Quality Building, Washington State University, Pullman, WA 99164, USA

gliadin proteins include amino acid sequences (epitopes) that can bind to specific human leukocyte antigen (HLA) receptors eliciting an immune response in people with CeD. This binding is recognized by gluten-sensitive T cell lymphocytes resulting in cytokine release and damage to the intestinal lining (Vader et al. 2002). Epitopes that result in consistently high immune responses in the majority of CeD patients are designated as immunodominant epitopes (e.g., DQ2.5-glia- $\alpha$ 1, DQ2.5-glia- $\alpha$ 2, DQ2.5-glia- $\omega$ 1, and DQ2.5-glia- $\omega$ 2) (Jabri and Sollid 2017; Tye-Din et al. 2010).

Multiple studies with children, including some with identical twins, have shown that the amount of consumed immunogenic wheat epitopes is a factor correlated with the incidence of CeD (Ivarsson et al. 2000; Mearin et al. 1983). In addition, people that carry the HLA-DQ8 allele have a lower risk of developing CeD than those carrying the HLA-DQ2 allele, which recognizes a larger number of epitopes than HLA-DQ8 (Megiorni et al. 2009). These results suggest that the quantity of ingested immunogenic epitopes may affect the onset of the disease (Koning 2012), and that a reduction of the immunogenic epitopes present in wheat may reduce the incidence of the disease at a population level.

However, elimination of all wheat immunogenic epitopes is a complex task since there are more than 40 unique CeD-toxic proteins currently known in the bread wheat genome (Chlubnova et al. 2023; Sollid et al. 2012, 2020). Moreover, deleting all the glutenin and gliadin proteins carrying CeD epitopes would result in unacceptable reductions in breadmaking quality. The elimination of immunogenic proteins with a limited contribution to breadmaking quality represents a practical intermediate step in the reduction of wheat CeD toxicity.

The  $\alpha$ -gliadins, located on the short arms of the chromosomes of homeologous group 6, are an attractive target for this initial step for a number of reasons. First,  $\alpha$ -gliadins are mostly monomeric proteins that typically do not form covalent bonds with the gluten polymer and are expected to have a limited effect on gluten strength. However, there are conflicting results on the effect of the deletion of  $\alpha$ -gliadins on breadmaking quality (Li et al. 2018; van den Broeck et al. 2009). In addition,  $\alpha$ -gliadins account for the greatest number of gliadins in the genomes of pasta wheat Svevo (68%) (Maccari et al. 2019) and bread wheat Fielder (55%) (Sato et al. 2021) and are the most abundantly expressed gliadins in the developing grains (Wang et al. 2017). More importantly, the  $\alpha$ -gliadins are particularly rich in known immunogenic nanomers (Chlubnova et al. 2023; Sollid et al. 2012, 2020) and larger peptides with multiple overlapping immunodominant epitopes (Anderson et al. 2000; Jabri and Sollid 2017; Shan et al. 2002).

We used gamma radiation to generate deletions encompassing the  $\alpha$ -gliadins in each of the three wheat genomes, which are designated hereafter as  $\Delta$ gli-A2,  $\Delta$ gli-B2, and

$\Delta$ gli-D2. In this study, we characterize the size of the deletions and their effect on grain yield, grain protein content, and breadmaking quality. Finally, we present proteomic results that explain the beneficial effects of the  $\Delta$ gli-D2 deletion on breadmaking quality relative to  $\Delta$ gli-A2 and  $\Delta$ gli-B2 deletions.

## Materials and methods

### Plant materials used in this study

The mutagenized line (RIL143, *Triticum aestivum* L. subsp. *aestivum*) is an  $F_7$ -derived  $F_8$  recombinant inbred line developed via single-seed descent from the cross between UC1110 and PI 610750. UC1110 is a hard white spring breeding line from the University of California, Davis (GRIN-Global accession GSTR 13501, pedigree Chukar/3/Yding//Bluebird/Chanate), and PI 610750 is a synthetic derivative from CIMMYT (PI 610750, pedigree: Croc1/Aegilops tauschii (Synthetic 205)//Kauz) (Lowe et al. 2011). RIL143 carries the adult plant stripe rust resistance gene *Yr34* (synonym *Yr48*) from PI 610750 and was mutagenized with gamma radiation as part of the efforts to fine map this resistance gene (Chen et al. 2021). We originally treated 2,076 grains with 300 GY of radiation from which we obtained 850 fertile  $M_1$  plants.  $M_2$  head rows were grown in the field at UC Davis in 2012–2013, and 650  $M_3$  head rows were grown in the field in 2013–2014, from which we harvested single spikes carrying the  $M_4$  seeds used in this study.

### Haplotype analysis

To select the best genome reference for each of the RIL143  $\alpha$ -gliadin loci, we performed a haplotype analysis. We used SNPs from the  $\alpha$ -gliadin genes and ten flanking genes on both sides of the gliadin region, extracted from the publicly available WheatCAP exome capture data in T3 (Blake et al. 2012) (<https://wheat.triticeaetoolbox.org/downloads/download-vcf.pl>, genotype trial 'Exome\_Capture\_2017\_WheatCAP\_UCD'). Based on Chinese Spring RefSeq v1.0 coordinates, the SNPs were extracted from chromosome 6A between 24,073,547 and 26,530,524 bp, from chromosome 6B between 42,773,234 and 45,164,040 bp, and from the unassigned chromosome between 93,797,403 and 94,934,120 bp. Most of the  $\alpha$ -gliadin genes within the Chinese Spring unassigned chromosome (ChrUn) belong to the D genome based on comparisons with Fielder and other sequenced genomes. Lines with more than 50% missing data were excluded from analysis. We performed a cluster analysis using R functions 'dist' and 'hclust' (method = 'ward.D2') (R-Core-Team 2021). Haplotypes were determined using 30% of the maximum clustering height.

After the haplotype analysis, we extracted 50 bp sequences flanking the informative SNPs and blasted them against 20 sequenced wheat genomes (Athiyannan et al. 2022; Kale et al. 2022; Maccafferri et al. 2019; Sato et al. 2021; Walkowiak et al. 2020; Zhu et al. 2019) and 5 *Aegilops tauschii* genomes (Luo et al. 2017; Zhou et al. 2021). SNPs were called based on the BLASTN results, combined with the previous SNPs, and used to repeat the clustering analysis using the same method as described above.

### Identification and characterization of the deletion lines

To identify deletions in  $\alpha$ -gliadin gene clusters on the short arms of chromosomes 6A, 6B, and 6D, we screened the RIL143 radiation mutants with genome-specific primers described in Table S1 and selected the ones with no PCR amplification. Final selected genotypes were verified using SDS-PAGE (Singh et al. 1991). We also developed primers to track a secondary deletion identified in chromosome 6A (primers Gap2F1 and Gap2R1, Table S1), and to confirm that this deletion was separated from  $\Delta gli$ -A2 in BC<sub>4</sub>F<sub>2</sub> plants selected from the introgression of  $\Delta gli$ -A2 into the variety Fielder. Finally, we intercrossed the  $\Delta gli$ -A2 and  $\Delta gli$ -D2 deletion lines and in the progeny selected a line homozygous for both deletions, designated hereafter as  $\Delta gli$ -A2  $\Delta gli$ -D2. Double deletions including  $\Delta gli$ -B2 were sterile.

To characterize the size of the deletions, we generated exome capture data using a previously described assay (Krasileva et al. 2017). Reads from the wild-type and mutant lines were mapped at high stringency (no SNPs allowed) to the Fielder reference genomes (v1.0) (Sato et al. 2021) using the BWA-MEM algorithm (Li 2013). Since reads mapped to multiple locations were split between locations, we used high stringency mapping to minimize the number of sequencing-reads from close homeologs mapping to reference genes in the deleted regions to establish more confident borders of the deletions. Genes with less than ten reads in the wild type were eliminated to minimize the effect of random fluctuations in calling deleted genes. We normalized the number of reads using the total number of reads and the length of the gene in kb and then calculated the ratio between the normalized reads/kb in the mutant relative to the wild type.

To test the effect of the  $\Delta gli$ -D2 deletion in a genetic background with higher yield potential and better bread-making quality than RIL143, we crossed the RIL143 line carrying the  $\Delta gli$ -D2 deletion with the commercial variety UC-Central Red (PVP 2019-00011). UC-Central Red is a high-yielding hard red spring wheat variety released by the University of California in 2021 that has excellent bread-making quality. We then backcrossed the F<sub>1</sub> four more times to UC-Central Red and in the progeny selected BC<sub>4</sub>F<sub>2</sub> plants

homozygous for  $\Delta gli$ -D2. The codominant simple sequence repeats (SSR) marker BARC54 linked to *GLI*-D2 (Table S1) was used to trace the deletion during the marker-assisted selection process.

### Growing conditions

The three single  $\alpha$ -gliadin deletion lines and the combined  $\Delta gli$ -A2  $\Delta gli$ -D2 deletion were compared to the non-mutagenized RIL143 in field experiments conducted at the UC Experimental Field Station in Davis, CA (38° 32' N, 121° 46' W) during the 2020–2021 and 2021–2022 growing seasons. The UC-Central Red sister lines with and without the  $\Delta gli$ -D2 deletion were evaluated in the same location during the 2021–2022 and 2022–2023 growing seasons. The soil at this location is a deep Yolo loam (fine-silty, mixed, superactive, nonacid, thermic Mollic Xerofluvent). Sowing was done in November at a density of 300 grains per m<sup>2</sup> (3 million grains per hectare) and managed with common agronomic practices. This included irrigations as needed and the application of ammonium sulfate fertilizer at the rate of 250 kg of N per hectare, half applied prior to planting and half applied at the late-tillering stage. Due to moderate stripe rust susceptibility of the RIL143 line, the field experiments were treated with foliar fungicides during the growing season.

### Breadmaking quality evaluations

We analyzed wheat quality at the California Wheat Commission Milling and Baking Laboratory (<http://californiawheat.org/>) using methods approved by the American Association of Cereal Chemists International (AACCI, Approved methods of analysis, 11th ed. AACCI Intl., St. Paul <http://methods.aaccnet.org/>). Before flour milling, 700 g of grain was tempered to 14% moisture and rested for 16–24 h. Milling extraction rates were calculated against total products and reported on an ‘as is’ moisture basis.

Measured traits included test weight (AACCI 55-10.1) and grain and flour protein (AACCI 46-30.01). Gluten rheological properties were evaluated using farinograph (AACCI 54-22.01), mixograph (AACCI 54-40.02) at the California Wheat Commission, and dough extensibility tests at the USDA-ARS Western Wheat Quality Laboratory using a Kieffer Dough Extensibility Rig on a TA.XT2i Texture Analyzer (Stable Micro Systems, Hamilton, MA, USA). The dough was prepared with 10 g of flour (14% moisture basis) mixed in a mixograph bowl to peak consistency. The program Texture Exponent (version 5.0.5.0) was used with the following settings: test mode = measure force in tension; option = return to start; pretest speed = 2.0 mm/s; test speed = 3.3 mm/sec; posttest speed = 10.0 mm/s; distance = 100 mm; and trigger force = auto at 5 g with 5 kg

load cell. Extensibility measurements were conducted using five replicates from an individual dough ( $n=5$ ). Finally, full baking tests were completed for all the samples (AACCI 10-12.01).

## Proteomic studies

We extracted wheat proteins from 500 mg of Chinese Spring flour using 10 mL of 50% 1-propanol. Under these conditions, the pellet is expected to include polymeric glutenins and linked gliadins, while the supernatant is expected to include monomeric gliadins and monomeric glutenins not incorporated into the macropolymer (Fig. S1). Samples were incubated in a 10 °C water bath and manually inverted every 10 min over the course of 1 h and centrifuged at 12,000×g at 10 °C for 30 min. The supernatant, which includes the propanol-soluble protein fraction, was lyophilized and ground to a fine powder. The precipitate was subjected to three consecutive washing steps to minimize the presence of proteins that were not covalently bound to the polymer. The washing steps included one wash with 50% 1-propanol at room temperature for 1 h plus one wash at 60 °C for 1 h. A final wash was performed with 2% SDS solution at 60 °C. Each washing step was followed by centrifugation and elimination of the supernatant. The final pellet was lyophilized and ground to a fine powder. Samples were then transferred to the UC Davis Proteomics Core Facility.

For each sample, 100 mg of wheat protein powder was solubilized into 5000 μL of solubilization buffer (5% SDS, 50 mM triethylammonium bicarbonate). This was placed inside tubes containing ceramic beads and homogenized with a MagNA Lyser instrument (Roche). The mix was centrifuged at 16,000×g, and the supernatant containing the solubilized proteins was saved. Volumes containing 150 μg total protein from each sample were reduced with dithiothreitol and alkylated with iodoacetamide in 50 mM triethylammonium bicarbonate (TEAB) buffer and then were sequentially digested with two enzymes via suspension-trap (S-Trap) devices (ProtiFi). The enzymatic digestion included first the addition of trypsin 1:100 enzyme/protein (wt/wt) for 4 h at 37 °C, followed by additional trypsin digestion using the same wt/wt ratios for overnight digestion at 37 °C. Samples were then subjected to digestion with chymotrypsin, adding the same wt/wt ratio as for the tryptic digest, for 6 h at 37 °C. Peptides were eluted from S-Trap by sequential elution buffers of 100 mM TEAB, 0.5% formic acid, 50% acetonitrile, and 0.1% formic acid. The eluted peptides were dried in a vacuum centrifuge and re-constituted in 0.1% trifluoroacetic acid.

Peptides were resolved on a Thermo Scientific Dionex UltiMate 3000 RSLC system using a PepSep analytical column (PepSep, Denmark): 150 μm × 8 cm C18 column with 1.5 μm particle size (100 Å pores), preceded by a

PepSep C18 guard column, and heated to 40 °C. Each injection included 0.6 μg of total peptide. Separation was performed in a total run time of 60 min with a flow rate of 500 μL/min, and mobile phases including: (A) water/0.1% formic acid and (B) 80% ACN/0.1% formic acid. Gradient elution was performed from 60 min = 4–10% B over 4 min, from 10 to 46% B over 44 min, 46–99% B in 1.5 min, down to 4% B in 0.5 min followed by equilibration for 5 min.

Peptides were analyzed on an Orbitrap Exploris 480 instrument (Thermo Fisher Scientific, Bremen, Germany). Spray voltage was set to 1.8 kV, funnel radio frequency level at 45, and heated capillary temperature at 275 °C. The full MS resolution was set to 60,000 at m/z 200, and full MS automatic gain control (AGC) target was 300% with the injection time set to Auto. Mass range was set to 350–1500. For fragmentation spectra, isolation width was set at 1.6 m/z and normalized collision energy was set at 30%. The AGC target value was set to Standard with max injection time of 40 ms and TopN = 30 scans.

Mass spectrometry raw files were processed with FragPipe, v.21.1 (Nesvizhskii, A. I. lab, University of Michigan). For all searches, we used a reference of curated prolamins and globulins (prol\_glob.gff3) from manually curated gene families from cultivar Chinese Spring ([https://urgi.versailles.inra.fr/download/iwgsc/IWGSC\\_RefSeq\\_Annotations/v1.1/](https://urgi.versailles.inra.fr/download/iwgsc/IWGSC_RefSeq_Annotations/v1.1/)) and the Uniprot FASTA, CRAp, of common laboratory contaminants. Precursor mass tolerance was set to  $\pm 20$  ppm and 25 ppm for fragments. Trypsin was specified as protease. A maximum of two missing cleavages were allowed, the required minimum peptide sequence length was 4 amino acids, and the peptide mass was between 300 and 5000 Da. Carbamidomethylation on cysteine (+57.021 Da) was set as static modification, and oxidation on methionine was set as dynamic modification (+15.995 Da). To determine and control the number of false-positive identifications, we used MsFagger to apply a target-decoy search strategy, using the concept of posterior error probability (PEP) to integrate multiple peptide properties, such as length, charge, and number of modifications into a single quantity reflecting the quality of a peptide spectral match. The reverse sequence library was used to control the false discovery rate (FDR) at less than 1% for peptide spectrum matches and protein group identifications. Decoy database hits, proteins identified as potential contaminants, and proteins identified exclusively by one site modification were excluded from further analysis. Label-free protein quantification was performed with the IonQuant algorithm v.10, but *Match Between Runs* feature (MBR) was disabled since each raw was submitted individually to FragPipe search. We accepted identifications with at least one unique peptide. Among the identified peptides, we focused on peptides diagnostic for the  $\alpha$ -gliadins with either seven (7-CYS) or six cysteines (6-CYS).

To estimate the effect of the  $\Delta gli\text{-}D2$  deletion on the relative abundance of gliadins and glutenins, we used a 50% 1-propanol extraction at room temperature and the trypsin–chymotrypsin digestion described above. Because the supernatants of 50% 1-propanol extractions include both gliadins and glutenins, we compared the spectral counts from this fraction in RIL143 and a  $\Delta gli\text{-}D2$  deletion line. We analyzed two independent pairs of samples from different replicates in the field experiment and determined the number of spectral counts for each annotated prolamin in each sample. Using these numbers, we estimated the changes caused by the  $\Delta gli\text{-}D2$  deletion on the percentage of glutenins (%-glutenins) relative to both the total gluten proteins and the total gluten proteins excluding the deleted  $\alpha$ -gliadins from the 6DS chromosome arm.

We estimated the proportion of  $\alpha$ -gliadin proteins lost in each deletion line relative to the wild type by adding the spectral counts from all the gliadins present in each locus. We used this information to estimate the expected proportional increases in the glutenin fraction (%-glutenins) and explored their relationships with gluten strength. To estimate gluten strength for each sample, we selected six quality parameters that reflect gluten strength and that were highly significant among genotypes: gluten index, farinograph development time and stability time, mixograph peak time, mixing peak height, and peak integral. To combine these six estimates, we first normalized the data by subtracting the mean of the trait and dividing by the standard deviation of the trait. We then averaged the six normalized values to obtain a single gluten score per sample. After confirming the significance of the regression between gluten strength score and predicted %-glutenins, we performed an analysis of covariance using predicted %-glutenin as covariate to test the differences between lines with and without the  $\Delta gli\text{-}D2$  deletion.

## Statistical analyses

Yield and quality analysis assays for RIL143 and UC-Central Red were analyzed using least-square means with years and blocks as random factors and blocks nested within years. Normality of residuals was checked using the Shapiro–Wilk test. When the hypothesis of normality of residuals was rejected, data were transformed to restore normality. Adjusted means for the wild type and mutants were compared using Dunnett multiple comparison tests. The field experiments including the RIL143 control and four deletion lines were grown for two years in a randomized complete block design (RCBD) with five replications, whereas those including the UC-Central Red sister lines with and without the  $\Delta gli\text{-}D2$  deletion were grown for two years in a complete randomized design (CRD) with six replications. Statistical analyses were performed using SAS v9.4 or R v4.4.2.

## Results

### Haplotype analysis of the *Gli2* region

To determine the closest sequenced wheat genomes to the *GLI-A2*, *GLI-B2*, and *GLI-D2* loci in RIL143, we performed haplotype analyses for each region using SNPs detected in the  $\alpha$ -gliadin genes and ten non-gliadin genes at each side of the *GLI2* loci. We generated exome capture data for RIL143 and compared it with exome capture data for 55 USA accessions obtained from the T3/Wheat database (WheatCAP project) and from 20 sequenced wheat genomes (Athiyanan et al. 2022; Avni et al. 2017; Maccaferri et al. 2019; Sato et al. 2021; Walkowiak et al. 2020).

The haplotype analysis for the 6A region (Fig. S2) revealed four haplotypes (HA1 to HA4), with HA1 and HA2 closer to each other and HA3 and HA4 clustered together (Table S2). The *GLI-A2* region from RIL143 was classified as haplotype HA1, which was also detected in the genomes of ArinaLrFor, Claire, Norin61, Robigus, and SY\_Mattis. Interestingly, the *GLI-A2* loci from available tetraploid (except Gredho) and spelt wheats clustered together in a separate haplotype (HA2).

The haplotype analysis for the 6B region (Fig. S3) revealed eight haplotypes (HB1 to HB8) clustered in two major groups. The first one included haplotypes HB4–HB6 and the second one the other 5 haplotypes (Table S3). The 6B region from RIL143 was included in the largest haplotype HB1, which was closest to the sequenced genomes of Kariega, Lancer, and Mace.

Finally, the haplotype analysis for the 6D region (Fig. S4), which includes SNPs from six sequenced *Ae. tauschii* genomes, revealed six haplotypes (HD1 to HD6). The *GLI-D2* region from RIL143 was included in haplotype H5, which was closer to the *Ae. tauschii* sequenced genomes than to the hexaploid wheat sequenced genomes, particularly in the region distal to the *GLI-D2* locus (Table S4). This result suggests that RIL143 6D region is either derived from a synthetic wheat, or that the HD2 haplotype is not present among the sequenced genomes by chance. Note that the *Gli-D2* region in CS RefSeq v1.0 and 2.0 is within the unassigned chromosome (Table S5).

Wheat cultivar Fielder is included in a different haplotype (HD2) than RIL143 based on the large number of SNPs in the region distal to *GLI-D2* but is more similar to RIL143 in the  $\alpha$ -gliadin sequences and the genes proximal to *GLI-D2* (Table S4). Six of the eight complete *GLI-D2* proteins identified in Fielder were identical to their orthologs in RIL143, and the other two showed only one non-synonymous SNP each (Q206H in TraesFLD6D01G062300 and S43P in TraesFLD6D01G062600). Because of this sequence similarity, we selected the

Fielder genome v1.0 as a reference for the *GLI-D2* gliadins in RIL143.

### Distribution of epitopes and cysteines in the alpha gliadin loci

Another reason for the selection of the Fielder genome as a reference was its better assembly of the *GLI2* loci. All three *GLI2* loci seem to be complete, with no  $\alpha$ -gliadins in the unassigned chromosomes. This better assembly likely reflects the improved technologies used to assemble the Fielder genome, which included long reads obtained with PacBio circular consensus sequencing using the HiFi approach (Sato et al. 2021). We manually curated the  $\alpha$ -gliadin genes from Fielder, and the corrections and comments are provided in Table S5. After curation, we identified eight complete gliadins in *GLI-A2*, fourteen in *GLI-B2*, and eight in *GLI-D2*.

We then characterized the number and location of the published lists of immunogenic nanomers (Chlubnova et al.

2023; Sollid et al. 2012, 2020) and larger immunogenic peptides (Anderson et al. 2000; Juhász et al. 2018; Shan et al. 2002) in each of the complete *GLI2*  $\alpha$ -gliadin proteins in Fielder (Fig. 1). These nanomers include the immunodominant peptides DQ2.5-glia- $\alpha$ 1a (PFPQPQLPY), DQ2.5-glia- $\alpha$ 1b (PYPQPQLPY), and DQ2.5-glia- $\alpha$ 2 (PQPQLPYPQ) that produce consistently high responses in the majority of CeD patients (Jabri and Sollid 2017). Of the 107 immunogenic epitopes detected in Fielder  $\alpha$ -gliadins, 55 (51.4%) are present in the *GLI-D2* locus (Table S5). The proportion is even larger among the immunodominant peptides, where 27 out of the 33 immunodominant epitopes (81.8%) are present in *GLI-D2*, 18.2% in *GLI-A2*, and none in *GLI-B2* (Table S5).

In addition to these immunogenic nanomers, two of the  $\alpha$ -gliadins in Fielder *GLI-D2* proteins (TraesFLD6D01G062600 and TraesFLD6D01G062700) contain a previously published 33-mer epitope that was shown to be highly immunogenic (Shan et al. 2002). This 33-mer includes six overlapping immunodominant nanomers and a 17-mer

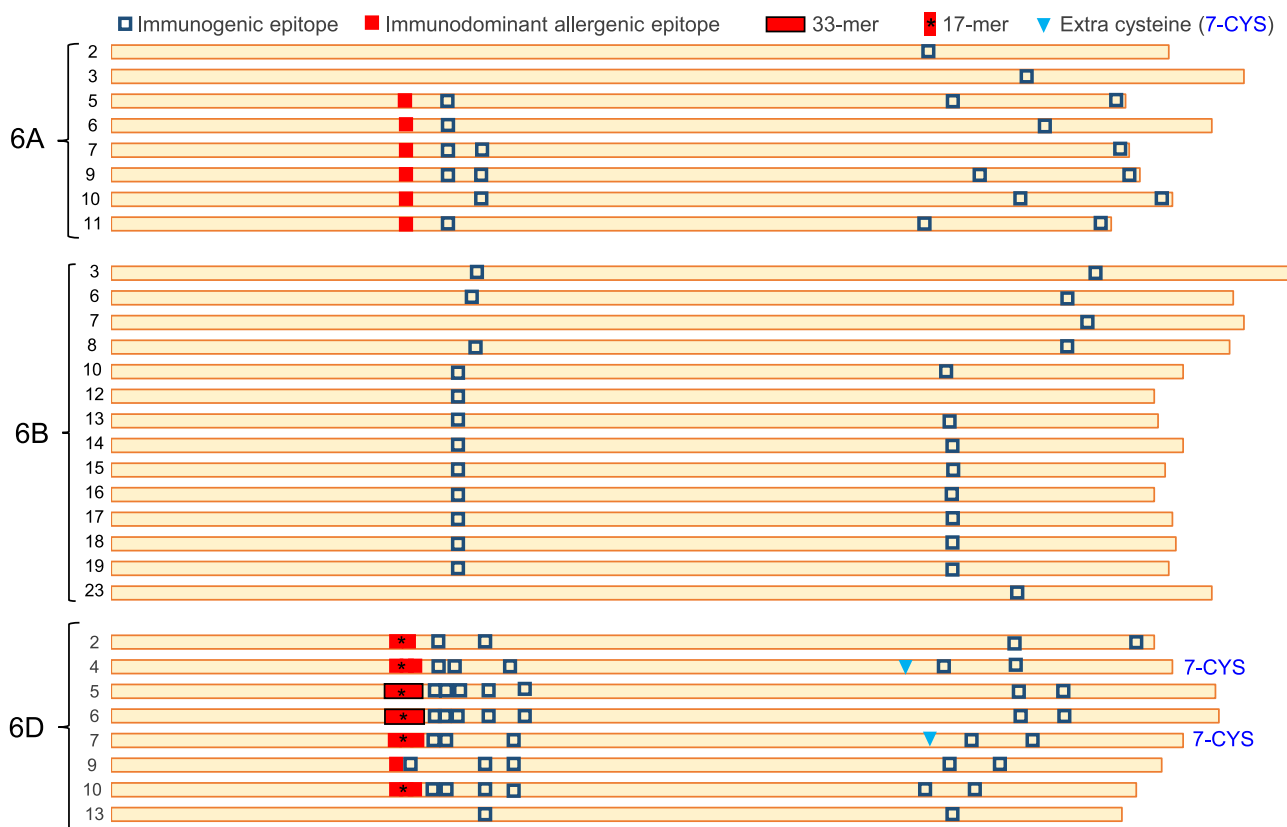


**Fig. 1** Complete  $\alpha$ -gliadin proteins from Fielder. All proteins showed six cysteines except for 6D-4 and 6D-7 (full gene names in Table S5), which have an additional cysteine indicated by triangles. Squares represent CeD immunogenic epitopes, with filled squares representing immunodominant epitopes and empty squares with dark borders less frequent epitopes (Chlubnova et al. 2023; Sollid et al.

2012, 2020). Adjacent epitopes appear as rectangles. Black borders around the overlapping filled squares indicate the presence of the immunodominant 33-mer including six overlapping immunodominant epitopes (Shan et al. 2002). The \* indicates the presence of the 17-mer within the immunodominant epitopes (Anderson et al. 2000)

immunodominant peptide (QLQPFPQPQLPYPQPQ(S/P/L)) (Anderson et al. 2000), which is also present in six out of the eight complete *GLI-D2* proteins in Fielder (Fig. 1, Table S5). These 17-mer and 33-mer immunogenic peptides are conserved in the orthologous *GLI-D2* proteins of RIL143, Chinese Spring, ArinaLrFor, and *Ae. tauschii* but were not detected in the *GLI-A2* or *GLI-B2* loci. Taken together, these results indicate that *GLI-D2* is the most immunogenic of the three  $\alpha$ -gliadins in hexaploid wheat.

The  $\alpha$ -gliadins from the *GLI-D2* locus from Fielder differ from those in the *GLI-A2* and *GLI-B2* loci by the presence of two  $\alpha$ -gliadins with an unusual number of cysteines (CYS). The number of CYS is important because it determines the ability of these proteins to form intra- or inter-protein disulfide bonds, with even numbers favoring intra-chain bonds and odd numbers favoring both intra- and inter-chain bonds (Masci et al. 2002). All the complete  $\alpha$ -gliadins found in the *GLI-A2* and *GLI-B2* loci in Fielder, ArinaLrFor, and Chinese Spring have six CYS located at relatively conserved distances (C-28/30-CC-11-C-76/119-C-7-C, Table S5). However, two to three of the *GLI-D2* gliadins in these genomes have a seventh cysteine between CYS-4 and CYS-5 (Fig. 1, Table S5). Orthologous 7-CYS gliadins are also present in *Ae. tauschii* *GLI-D2* locus, indicating that these unusual gliadins were contributed by the diploid donor of the D genome. Based on their similarity with the *Ae. tauschii* and Fielder sequences, we were able to assign the 7-CYS  $\alpha$ -gliadins present in the unassigned chromosome in Chinese Spring and ArinaLrFor to the *GLI-D2* locus. Using D genome-specific primers and the  $\Delta gli-D2$  deletion, we also confirmed that the 7-CYS  $\alpha$ -gliadins from RIL143 are present in the 6D chromosome.

## Determination of the size of the radiation mutants with *GLI2* deletions

The PCR screening of the RIL143 radiation mutants with *GLI2* genome-specific primers (Table S1) yielded one line with a deletion in *GLI-A2* ( $\Delta gli-A2$ ), three with deletions in *GLI-B2* ( $\Delta gli-B2$ ), and three with deletions in *GLI-D2* ( $\Delta gli-D2$ , Fig. 2). Polyacrylamide gel electrophoresis of the alcohol-soluble grain proteins from these lines showed the three  $\Delta gli-B2$  deletions shared the same missing bands, and the same was true for the three  $\Delta gli-D2$  deletions (Fig. 2). We selected one line for each of the three deleted loci and estimated the size of the deletions using exome capture.

We used the coordinates of the Fielder genes flanking the borders of the deletions to estimate the minimum and maximum possible sizes of the deletions and the number of deleted gliadins and flanking genes (Table 1 and Fig. 3). We mapped the exome capture reads to the Fielder reference at high stringency and eliminated genes with less than 10 reads to minimize the effect of random

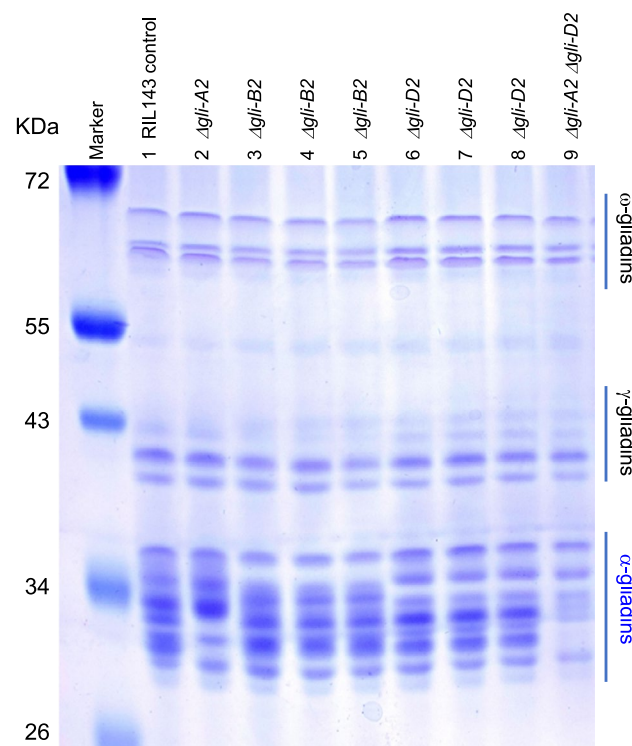


**Fig. 2** Polyacrylamide gel showing soluble proteins extracted with 50% 1-propanol. Note the different  $\alpha$ -gliadins missing in the *GLI-A2* (6A), *GLI-B2* (6B), and *GLI-D2* (6D) deletions. Some homoeologous bands overlap with each other, and their deletion is only clear in the line carrying the 6A and 6D deletions (lane 9)

fluctuations. We normalized the read count using the total number of reads and gene size (see Materials and Methods) and calculated the ratio between mutant and WT normalized reads. This ratio is expected to be close to 1 outside the deletion and close to 0 inside the deletion.

Using this method, we estimated that the  $\Delta gli-A2$  deletion is between 4.2 and 5.1 Mb long (Table 1, Fig. 3, Table S6). This deletion includes all eight complete gliadins in *GLI-A2* and 67–73 other high-confidence annotated genes. We also mapped the exome capture reads of the RIL143 6A deletion to the closest genome of ArinaLrFor (Fig. S2, Table S2), which has an expanded *GLI-A2* locus with 14 complete gliadins. This analysis confirmed that all 6A  $\alpha$ -gliadins in RIL143 were deleted.

The RIL143 line carrying the  $\Delta gli-A2$  deletion has a secondary deletion located ~ 95.6 Mb proximal to  $\Delta gli-A2$  and estimated to be 20.1 to 22.5 Mb long, based on Fielder genome coordinates (Table 1, Fig. 3, Table S6). We developed primers to detect the secondary deletion in 6A (Gap2F1 and Gap2R1, Table S1) and used them to test recombination events between the two deletions. Using these primers, we found that the secondary deletion was no longer present in a Fielder line in which we backcrossed the  $\Delta gli-A2$  deletion for four generations. This result

**Table 1** Characterization of radiation mutants that eliminate  $\alpha$ -gliadins from chromosome arms 6AS, 6BS, and 6DS

| Fielder Coordinates               | $\Delta gli$ -A2 | 6AS 2nd deletion | $\Delta gli$ -B2 | $\Delta gli$ -D2 |
|-----------------------------------|------------------|------------------|------------------|------------------|
| Distal                            | 26,602,986       | 125,796,709      | 47,591,785       | 17,837,748       |
| Border                            | 27,500,174       | 127,291,438      | 47,799,566       | 19,674,383       |
| Proximal                          | 31,661,530       | 147,364,040      | 49,980,150       | 34,361,047       |
| Border                            | 31,710,947       | 148,295,698      | 50,229,076       | 34,738,339       |
| Size del. in Mb                   | 4.16–5.11        | 20.07–22.50      | 2.18–2.63        | 14.69–16.90      |
| <i>Gli2</i> excluding pseudogenes | 8                | 0                | 14               | 8                |
| Total non- <i>Gli2</i> genes      | 79               | 93               | 24               | 262              |
| Gliadins outside deletion         | 0                | NA               | 1                | 0                |

demonstrates that these two deletions can be separated by recombination.

The  $\Delta gli$ -B2 deletion was estimated to be between 2.2 and 2.6 Mb based on the Fielder genome coordinates (Table 1, Fig. 3, Table S6) and includes 13 of the 14 complete *GLI*-B2 gliadins. The only exception is *TraesFLD6B01G102300*, which encodes an  $\alpha$ -gliadin located 17 Mb proximal to the major *GLI*-B2 cluster (at 67.4 Mb, Table 1 and Table S6). We confirmed that the RIL143 gene orthologous to *TraesFLD6B01G102300* was still present in the  $\Delta gli$ -B2 deletion using gene-specific primers (Table S1) and Sanger sequencing. In addition to the 13 missing gliadins, the  $\Delta gli$ -B2 deletion includes 25–29 other high-confidence annotated genes.

Finally, we estimated that the 6D deletion in RIL143 is between 14.7 and 16.9 Mb long. The eight complete gliadins in this locus are all included in the deletion as well as other 259–267 annotated genes (Table 1, Fig. 3, Table S6). We intercrossed the three different  $\alpha$ -gliadin deletions, but only the  $\Delta gli$ -A2  $\Delta gli$ -D2 combined deletion was fertile (Fig. 2, lane 9). Combinations of  $\Delta gli$ -B2 with any of the other two deletions resulted in plants with no anthers and multiple pistils that yielded no seeds (Fig. S5). No plants with all three deletions were recovered.

We hypothesized that one or more genes within the overlapping region among these deletions could be responsible for the observed phenotype. We did not prioritize the region proximal to the *GLI2* locus because the proximal border of the  $\Delta gli$ -A2 deletion coincides with the border of the gliadin cluster, and no genes proximal to *GLI*-A2 are deleted (Table S6). Therefore, we focused on the twelve genes distal to the *GLI*-B2 locus that are deleted in  $\Delta gli$ -B2, which is smaller than the number of genes distal to  $\Delta gli$ -D2 (Table S7). The annotations of these wheat genes and their rice and Arabidopsis homologs did not yield any obvious candidate gene for the flower phenotype, so mutants or other functional studies will be required to identify the causal genes.

The three RIL143 individual deletions have been deposited in GRIN-Global and are publicly available without

restrictions under germplasm accession numbers PI 704906 ( $\Delta gli$ -A2), PI 704907 ( $\Delta gli$ -B2), and PI 704908 ( $\Delta gli$ -D2).

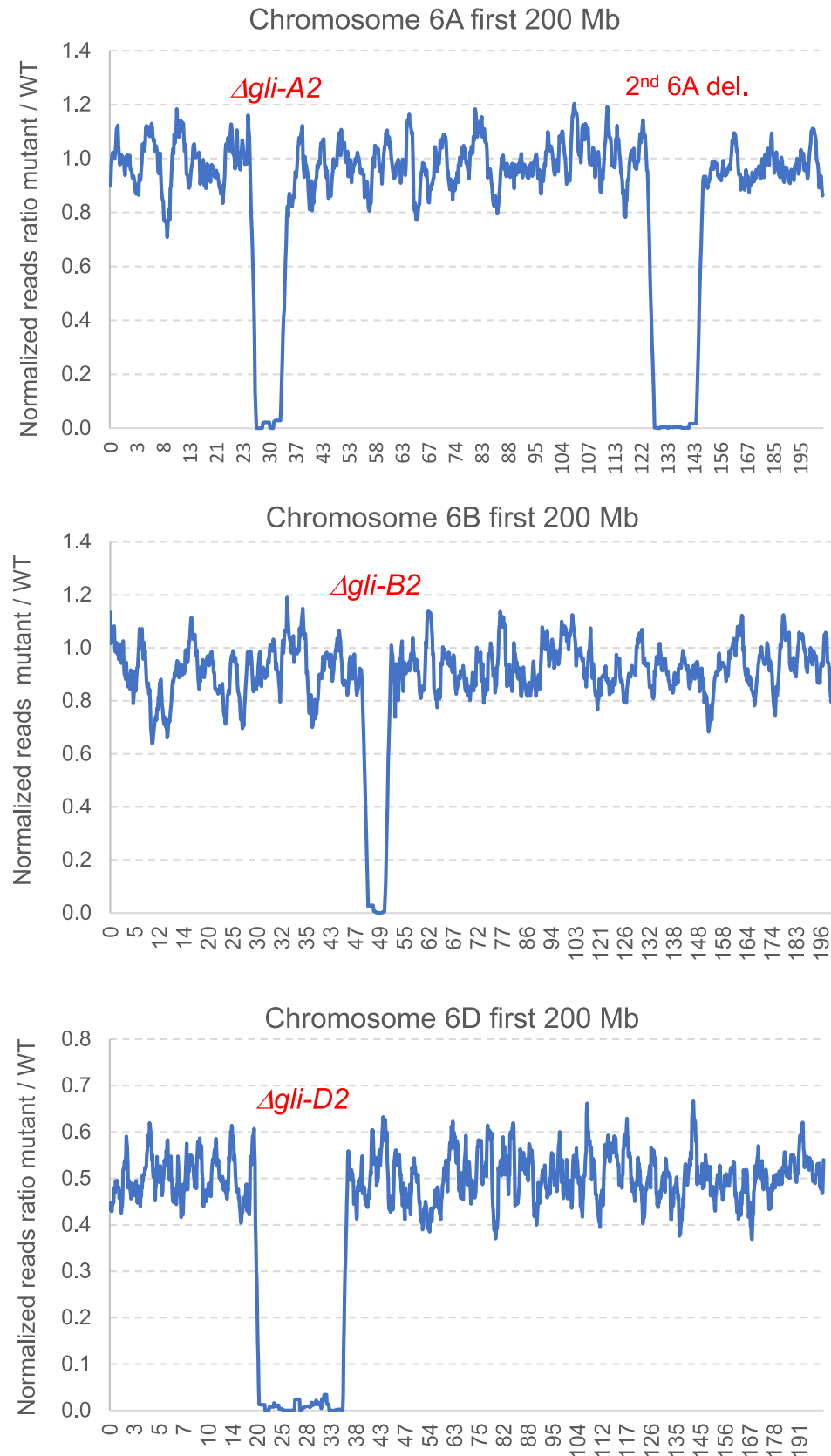
### Yield and agronomic field performance of the deletion lines

To determine the practical value of the deletions, we evaluated the effects of  $\Delta gli$ -A2,  $\Delta gli$ -B2,  $\Delta gli$ -D2, and combined  $\Delta gli$ -A2  $\Delta gli$ -D2 relative to RIL143 on agronomic performance in field experiments. Figure 4 presents the adjusted least-square means across two years for grain yield (kg/ha, Fig. 4A), thousand kernel weight (g, Fig. 4B), test weight (kg/hl, Fig. 4C), and percent grain protein content (at 12% moisture, Fig. 4D). Additional data are available for plant height and heading time in supplemental Table S8 (RIL143).

In general, the *GLI2* deletion lines showed non-significant differences from the wild-type RIL143 for all the traits described above (Fig. 4, Table S8). One exception was an average 19% decrease in grain yield in the  $\Delta gli$ -A2 deletion, which was marginally significant in the Dunnett test ( $P < 0.05$ , Fig. 4A). The  $\Delta gli$ -D2 deletion showed slightly higher yields than the control but the differences were not significant. A slightly favorable effect of  $\Delta gli$ -D2 was also observed in the combined  $\Delta gli$ -A2  $\Delta gli$ -D2 deletions, which no longer showed the significant yield reduction detected in the  $\Delta gli$ -A2 deletion alone (Fig. 4A). The combined  $\Delta gli$ -A2  $\Delta gli$ -D2 deletion also showed a significant reduction in plant height (Table S8), and a marginally significant effect on test weight ( $P < 0.05$ , Fig. 4C). However, the 1.2% increase in test weight is likely not agronomically relevant.

Since RIL143 is not a commercial variety and has limited yield potential and intermediate breadmaking quality, we introgressed the  $\Delta gli$ -D2 deletion in the high-yielding and high-quality commercial line UC-Central Red by four backcrosses using the linked microsatellite marker BARC54 (Table S1). We initially focused on the  $\Delta gli$ -D2 deletion because it eliminates a significantly higher proportion of regular and immunodominant epitopes than the  $\Delta gli$ -A2 and  $\Delta gli$ -B2 deletions (Fig. 1). Additional data for plant height

**Fig. 3** Graphical representation of the radiation deletions  $\Delta gli\text{-}A2$ ,  $\Delta gli\text{-}B2$ , and  $\Delta gli\text{-}D2$  using an overlapping moving window of ten genes (only first 200 Mb shown). A secondary deletion was detected on chromosome 6A. The values in the x-axis indicate the coordinates in Mb in the Fielder chromosomes



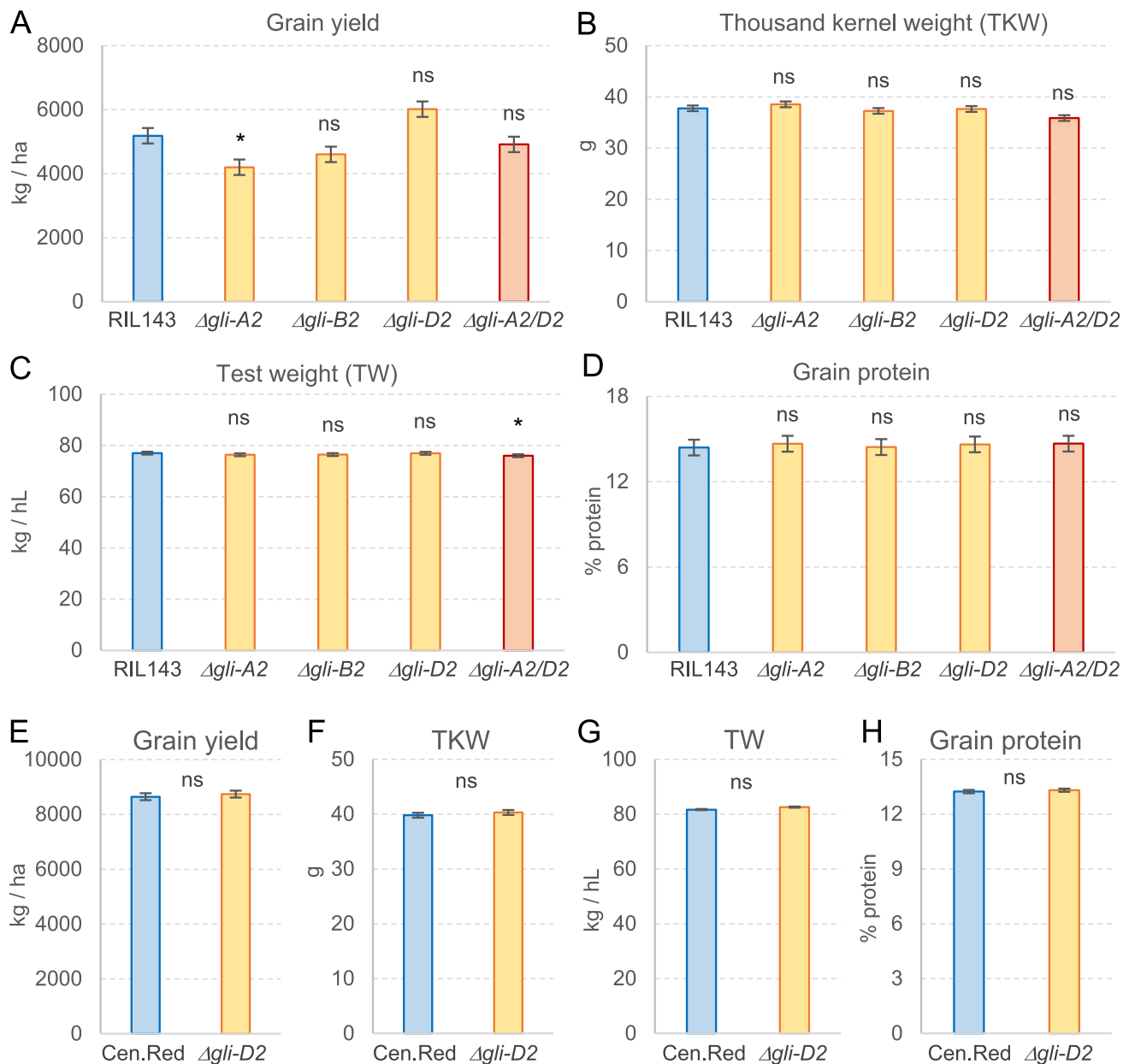


**Fig. 4** Field evaluation of RIL143 and UC-Central Red sister lines with and without *GLI2* deletions. **A–D** RIL143 and lines with deletions in chromosomes 6A ( $\Delta$ gli-A2), 6B ( $\Delta$ gli-B2), 6D ( $\Delta$ gli-D2), and both 6A and 6D ( $\Delta$ gli-A2  $\Delta$ gli-D2) ( $n=5$  each year). Adjusted means of the deletion lines were compared with the wild-type RIL143 using Dunnett tests. **(E–H)** UC-Central Red and its sister

line with the  $\Delta$ gli-D2 deletion ( $n=6$  each year). Bars are least-square means for the combined years, and error bars are standard errors of the means (s.e.m.).  $P$  values are based on ANOVAs combining two years of field data, using years as blocks. ns, not significant,  $*P<0.05$ . Raw data and statistical tests are available in Table S8 for A–D and Table S9 for E–H

and heading time for UC-Central Red are listed in Table S9. Similar to RIL143 deletion lines, the UC-Central Red sister lines with and without the  $\Delta$ gli-D2 deletion showed no significant differences in grain yield (Fig. 4E), thousand kernel weight (Fig. 4F), test weight (Fig. 4G), grain protein content (Fig. 4G), plant height or heading time (Table S9). Taken together, these data suggest that the introgression of

the  $\Delta$ gli-D2 deletion can be a useful tool for common wheat breeding programs.

#### Breadmaking quality evaluation of the radiation mutants

In contrast with the limited effects of the  $\alpha$ -gliadin deletions on agronomic performance, we observed highly

significant effects on breadmaking quality. In RIL143, these effects were larger in the  $\Delta gli\text{-}D2$  and combined  $\Delta gli\text{-}A2 \Delta gli\text{-}D2$  deletions and smaller or not significant in the  $\Delta gli\text{-}A2$  and  $\Delta gli\text{-}B2$  deletions (Fig. 5A–F, Table S10). Relative to RIL143, the  $\Delta gli\text{-}D2$  deletion increased gluten index by 24% (Fig. 5A), farinograph stability by 129% (Fig. 5B), mixing peak time by 53% (Fig. 5C), mixograph peak integral by 59% (Fig. 5D), bread loaf volume by 12% (Fig. 5E), and overall baking score by 65% (Fig. 5F, Table S10). The combined  $\Delta gli\text{-}A2 \Delta gli\text{-}D2$  deletion

showed similar beneficial effects on breadmaking quality as the single  $\Delta gli\text{-}D2$  deletion (Fig. 5A–F).

In addition to the parameters shown in Fig. 5A–F, the  $\Delta gli\text{-}D2$  and combined  $\Delta gli\text{-}A2 \Delta gli\text{-}D2$  deletion lines showed significant and positive effects on farinograph water absorption (4–5%), development time (62–72%), and mixing peak height (7%). Both deletion lines also exhibited beneficial effects in several baking tests including water absorption (4–5%), mixing time (16–31%), dough handling (133–150%), crumb grain (49–62%), and bread symmetry

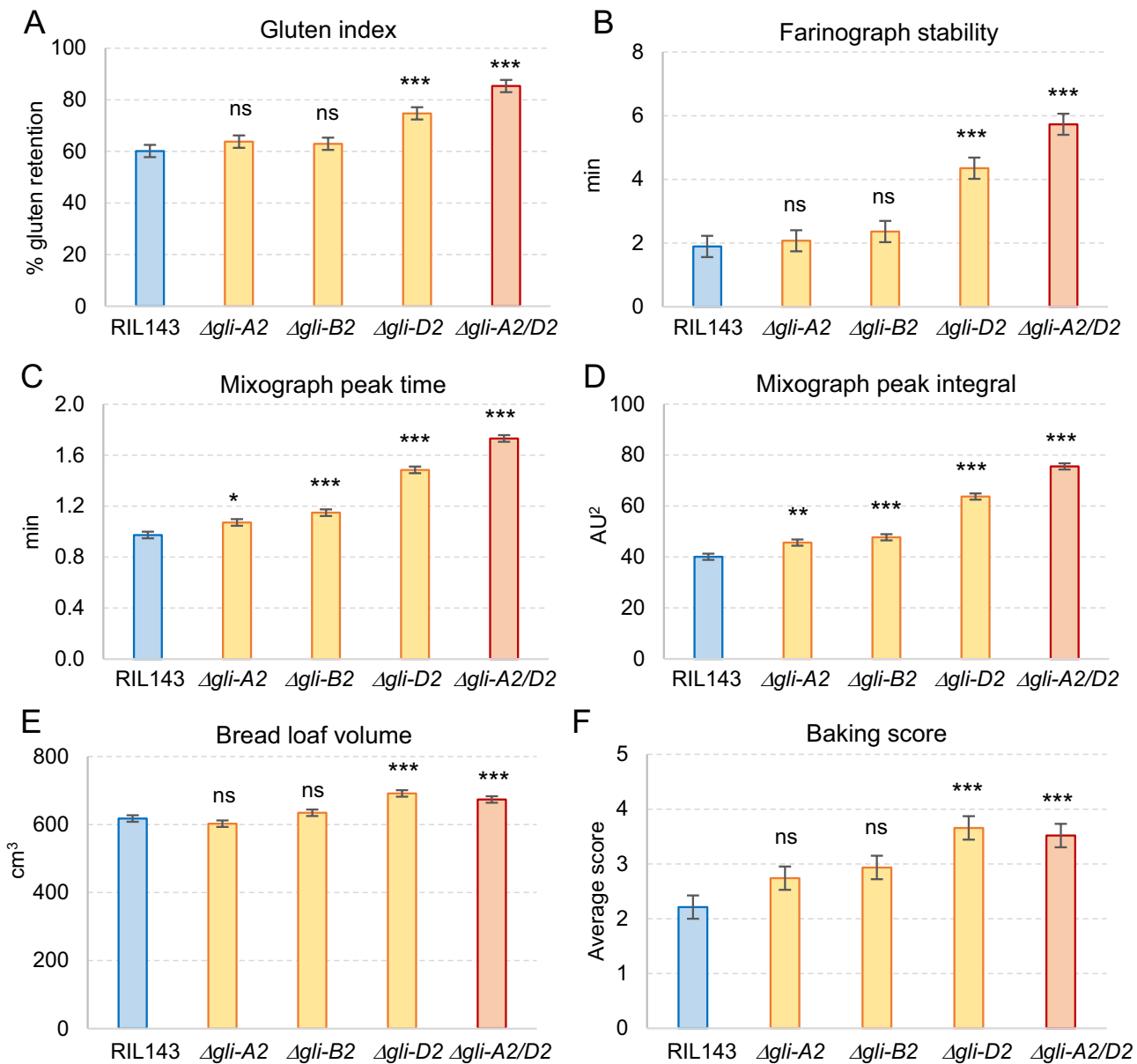


**Fig. 5** Breadmaking quality evaluation of RIL143 sister lines with and without *GLI2* deletions. **A–F** RIL143 and lines with deletions in chromosomes 6A ( $\Delta gli\text{-}A2$ ), 6B ( $\Delta gli\text{-}B2$ ), 6D ( $\Delta gli\text{-}D2$ ), and both 6A and 6D ( $\Delta gli\text{-}A2 \Delta gli\text{-}D2$ ) ( $n=5$  in 2021 and 4 in 2022). Adjusted means of the deletion lines were compared with the wild-

type RIL143 using ANOVA and Dunnett tests. The two years of field trials were used as blocks. Bars are adjusted least-square means across years, and error bars are standard errors of the adjusted means (s.e.m.). ns, not significant,  $*P < 0.05$ ,  $**P < 0.01$ ,  $***P < 0.001$ . Raw data and statistical tests are available in Table S10

(80–86%, Table S10), which explains the large increase in overall baking score. The only negative effect was a 2–4% reduction in flour yield for the combined  $\Delta gli$ -A2  $\Delta gli$ -D2 deletion, which was not significant in the single  $\Delta gli$ -D2 deletion. This parameter was also marginally significant for  $\Delta gli$ -A2 and  $\Delta gli$ -B2 ( $P < 0.05$ ).

To test if the gliadin deletions affected dough extensibility, we established a collaboration with the USDA-ARS Western Wheat Quality Laboratory in Pullman, WA, to analyze flour samples from the 2022 field experiment (Fig. S6 and Table S10). Results from the extension tests showed no significant difference in distance to break between RIL143 and its four sister deletion lines (Fig. S6A, Table S10), indicating no significant changes in dough extensibility. Conversely, the force at break (a measure of gluten strength) showed significantly higher force values for the  $\Delta gli$ -D2 and combined  $\Delta gli$ -A2  $\Delta gli$ -D2 deletions than for the  $\Delta gli$ -A2 or  $\Delta gli$ -B2 single deletion lines (Fig. S6B, Table S10). The latter results confirmed the positive effect of the  $\Delta gli$ -D2 deletion on gluten strength.

The UC-Central Red line with the  $\Delta gli$ -D2 deletion also showed positive and highly significant effects for gluten index (7.5%, Fig. 6A), farinograph stability (47.4%, Fig. 6B), mixograph mixing peak time (31.2%, Fig. 6C), and mixograph peak integral (33.9%, Fig. 6D, Table S11). Among the baking quality tests, the  $\Delta gli$ -D2 deletion in UC-Central Red was also associated with positive and significant effects on mixing time (8.8%, Fig. 6E) and dough handling (13.3%, Fig. 6F). Loaf volume (1.2%, Fig. 6G) and baking score (7.2%, Fig. 6H) were slightly higher in the  $\Delta gli$ -D2 deletion than in the UC-Central Red control, but the increases were not significant (Table S11). The  $\Delta gli$ -D2 line also showed a 4.5% higher sedimentation test than UC-Central Red, confirming the beneficial effect of  $\Delta gli$ -D2 on gluten strength. However, the relative increases in gluten strength in UC-Central Red were smaller than those in RIL143, likely because the baseline values were higher in the commercial variety. These results indicate that the  $\Delta gli$ -D2 deletion can also benefit bread wheat lines with good breadmaking quality. The only negative effect

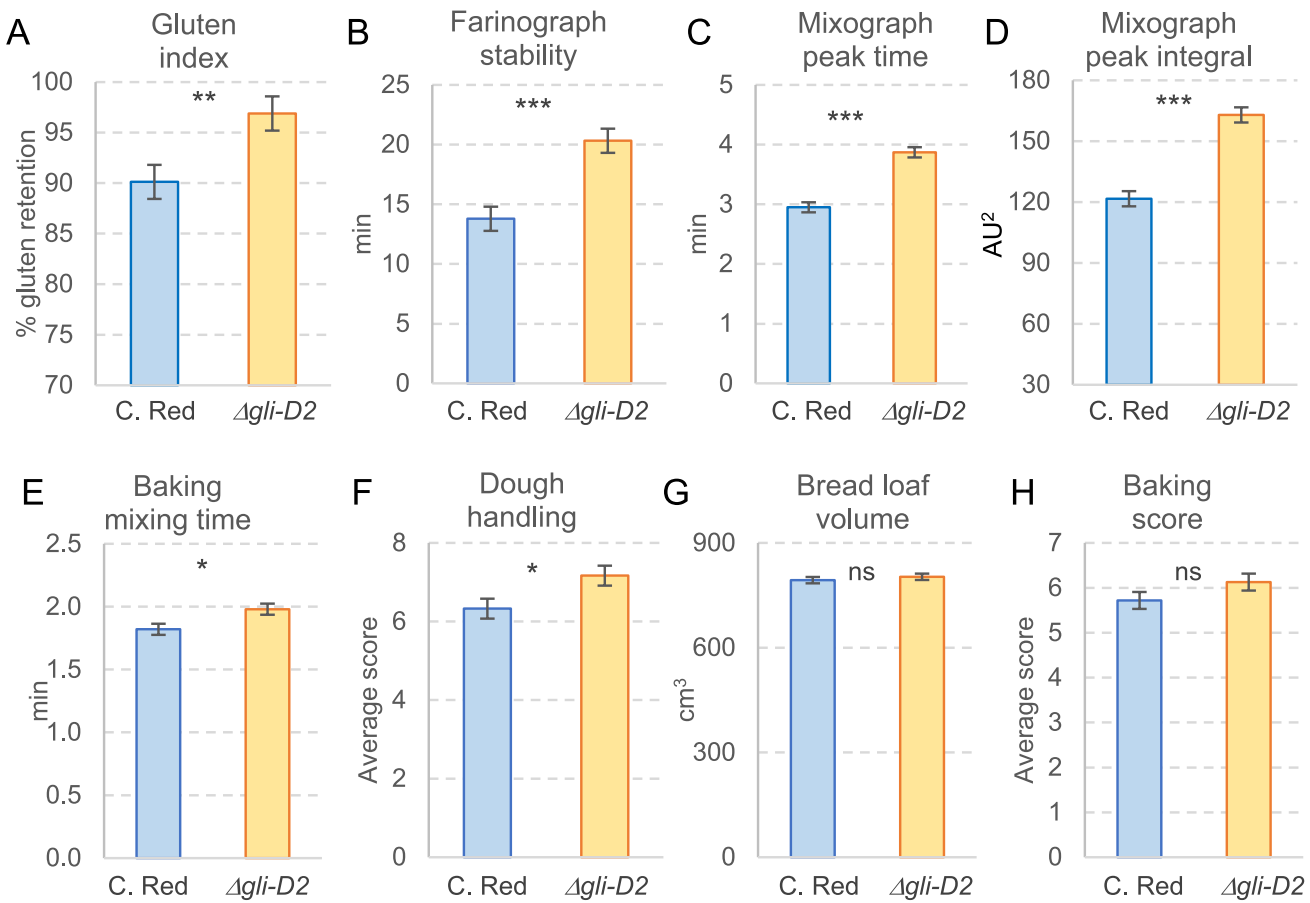


**Fig. 6** Breadmaking quality evaluation of UC-Central Red sister lines with and without the  $\Delta gli$ -D2 deletion. ( $n = 6$  each year). Adjusted means were compared using ANOVA with years as blocks. Bars are

adjusted least-square means across years, and error bars are standard errors of the adjusted means (s.e.m.). ns, not significant, \*\* $P < 0.01$ , \*\*\* $P < 0.001$ . Raw data and statistical tests are available in Table S11

of  $\Delta gli\text{-}D2$  in UC-Central Red was a marginally significant decrease (9%,  $P=0.02$ ) in total wet gluten (Table S11).

In summary, the  $\Delta gli\text{-}D2$  deletion was associated with beneficial effects on gluten strength and breadmaking quality in genetic backgrounds with contrasting initial quality parameters.

### $\alpha$ -gliadins with 7 cysteines are frequently incorporated in the gluten polymer

The previous results indicate that one or more genes located within the  $\Delta gli\text{-}D2$  deletion have a negative impact on gluten strength in the wild type, and that those genes are likely different from their orthologs within the  $\Delta gli\text{-}A2$  and  $\Delta gli\text{-}B2$  deletions. Since only the  $GLI\text{-}D2$  locus includes 7-CYS  $\alpha$ -gliadins, we hypothesized that these gliadins form disulfide bonds with the gluten polymer, acting as chain terminators and reducing the gluten polymer length and strength.

To test this prediction, we separated proteins soluble in 50% 1-propanol from the gluten polymer by centrifugation and thoroughly washed the gluten polymer to eliminate proteins that were not covalently linked to the gluten polymer. We digested protein fractions with trypsin and chymotrypsin and analyzed the resulting fragments by mass spectrometry (see Materials and Methods).

We aligned the 7-CYS and 6-CYS  $\alpha$ -gliadins and identified several amino acid polymorphisms that were diagnostic for the two groups (Fig. S7). We then focused on peptides carrying these diagnostic polymorphisms, including five for the 7-CYS  $\alpha$ -gliadins and 18 for the 6-CYS  $\alpha$ -gliadins (Table 2 and Fig. S8). We performed two experiments, and since they showed consistent results, we combined them for statistical analyses (Table 2).

Of the 15 spectral counts of peptides that mapped exclusively to 7-CYS  $\alpha$ -gliadins, 26.7% were detected in the propanol-soluble fraction, and the remaining 73.3% were present in the pelleted fraction. By contrast, of the

**Table 2** Frequency of  $Gli\text{-}D2$  digested peptides in the alcohol-soluble and insoluble fractions of gluten

| Peptide sequence                                | Experiment 1 |        | Experiment 2 |        | Combined |        |
|---|--------------|--------|--------------|--------|----------|--------|
|   | Solution     | Pellet | Solution     | Pellet | Solution | Pellet |
| <i>7C specific</i>                              |              |        |              |        |          |        |
| HQQQQQQQQQQPL                                   | 0            | 1      | 1            | 1      | 1        | 2      |
| QQSQQQYPSGQGSFQPSQQNPQAQGSVQPQQLPQFEEIR         | 0            | 0      | 2            | 2      | 2        | 2      |
| MQLQPFPQPKLPYPPQQLPYPQPKPQPF                    | 0            | 0      | 0            | 1      | 0        | 1      |
| VQQQQFPGQQQPFPPQQPYPQLQPFPSQQPY                 | 0            | 0      | 0            | 1      | 0        | 1      |
| RPQQSYQPQPKQY                                   | 0            | 2      | 1            | 3      | 1        | 5      |
| Total N of peptides in 7-CYS $\alpha$ -gliadins | 0            | 3      | 4            | 8      | 4        | 11     |
| <i>6C specific</i>                              |              |        |              |        |          |        |
| QQQQLIPCR                                       | 2            | 0      | 1            | 0      | 3        | 0      |
| VPVPQLQPQNPSLQQPQEQQVPL                         | 2            | 2      | 2            | 2      | 4        | 4      |
| QQPQQQYPSGQGSFQPSQQNPQAQGSVQPQQLPQFEEIR         | 5            | 0      | 5            | 2      | 10       | 2      |
| FQPSQQNPQAQGSF                                  | 0            | 0      | 1            | 0      | 1        | 0      |
| IPPYCTIAPF                                      | 0            | 0      | 2            | 1      | 2        | 1      |
| LQLQPFPQPKLPYPPQPKP                             | 2            | 0      | 1            | 1      | 3        | 1      |
| NLALQTLPAMCNVY                                  | 1            | 0      | 2            | 1      | 3        | 1      |
| QPQQLPQFEAIR                                    | 0            | 1      | 0            | 0      | 0        | 1      |
| QQPQQQYPSGQQGF                                  | 10           | 0      | 2            | 2      | 12       | 2      |
| VPVPQLQL  | 0            | 0      | 1            | 0      | 1        | 0      |
| VPVPQLQLQNPSQQPQEQQVPL                          | 2            | 0      | 2            | 1      | 4        | 1      |
| HQQQQQQQQQQQQQQPL                               | 1            | 0      | 2            | 1      | 3        | 1      |
| HHHQQQQQQPSSQVSY                                | 0            | 0      | 1            | 0      | 1        | 0      |
| QQPQEQQYPSGQGSFQSSQQNPQAQGSVQPQQLPQFQEIR        | 2            | 0      | 0            | 0      | 2        | 0      |
| QSSQQNPQAQGSVQPQQLPQFQEIR                       | 0            | 0      | 2            | 0      | 2        | 0      |
| DVVLQQHNIAHGSSQVLQESTY                          | 0            | 2      | 0            | 0      | 0        | 2      |
| RPQQPYQPQSQPQYSPQQPQPISSQQQQQQQQQQQQK           | 2            | 0      | 2            | 1      | 4        | 1      |
| RPQQPYQPQSQPQYSPQQPQPISSQQQQQQQQQQQQK           | 1            | 0      | 2            | 0      | 3        | 0      |
| Total N of peptides in 6-CYS $\alpha$ -gliadins | 30           | 5      | 28           | 12     | 58       | 17     |
| Fisher's exact test two-sided $P$ value         | 0.0066       |        | 0.0401       |        | 0.0003   |        |

75 spectral counts of peptides diagnostic for the 6-CYS  $\alpha$ -gliadins, 77.3% were detected in the propanol-soluble fraction and the remaining 22.7% in the pellet (Table 2). A two-sided exact Fisher test confirmed a highly significant departure from an independent distribution of the 7-CYS and 6-CYS peptides in the two fractions ( $P=0.0003$ ).

In the pellet fraction, the 3.2-fold enrichment of the 7-CYS (73.3%) relative to the 6-CYS peptides (22.7%) was similar to the 2.8-fold enrichment of the HMW-GS peptides (54.2%) relative to  $\alpha$ -gliadins from the A and B genomes (19.3%, all 6-CYS). Taken together, these results indicate that the 7-CYS  $\alpha$ -gliadins are incorporated into the gluten macropolymer more frequently than the 6-CYS  $\alpha$ -gliadins, which are predominantly found in the propanol-soluble phase.

### The $\Delta gli$ -D2 deletion affects both the presence of 7-CYS $\alpha$ -gliadins and the overall proportion of glutenins

The presence of  $\alpha$ -gliadins with 7-CYS in the  $GLI$ -D2 locus and their absence in the  $GLI$ -A2 and  $GLI$ -B2 loci provide a possible explanation for the observed increases in gluten strength in the lines carrying the  $\Delta gli$ -D2 deletion relative to the other genotypes. However, gliadin deletions can increase the proportion of glutenins over the total proteins (%-glutenins), which can also contribute to gluten strength. To estimate this contribution, we performed a proteomics analysis of digested proteins extracted from the wild-type RIL143 and the  $\Delta gli$ -D2 deletion (see Materials and Methods).

As expected, the 6D- $\alpha$ -gliadins showed a highly significant decrease in spectral counts in  $\Delta gli$ -D2 relative to RIL143. However, this decrease was not 100% because peptides from GLI-A2 or GLI-B2 that are identical to GLI-D2 are also counted for the GLI-D2 reference. To explore the effect of  $\Delta gli$ -D2 on the relative abundance of other proteins, we excluded the spectral counts from the 6D- $\alpha$ -gliadins from the initial analyses. When these proteins were excluded, the differences between RIL143 and  $\Delta gli$ -D2 for the ratio between glutenins and gliadins and the %-glutenins were small and in opposite directions in the two samples (Table S12), suggesting the absence of significant differences. These results, together with the absence of significant differences in total grain proteins among genotypes (Table S8), suggest that the resources not used by the deleted gliadins are distributed proportionally among the remaining prolamins.

However, when the %-glutenins were calculated as a fraction of the total spectral counts including the 6D- $\alpha$ -gliadins, the values for the two samples were consistently higher in the  $\Delta gli$ -D2 deletion (average 56.1%) than in the wild type (53.5%, Table S12). Although we did not perform proteomics experiments for the other deletions, we were able

to estimate their expected increases in %-glutenins by using the relative spectral counts of the three  $GLI$  loci calculated in Table S12, and a proportional distribution of resources released in the deletion lines (Table S13). As a baseline for the calculation of the predicted increases in %-glutenins, we used an average of previously published proportions of glutenins (35%) and gliadins (65%) in common wheat (Wieser et al. 2022).

We used the predicted increases in %-glutenin in each line to visualize their effects on gluten strength. An average gluten strength score was estimated for each sample using the average of six normalized quality parameters (Table S13). These parameters are known to be associated with gluten strength, and all exhibited highly significant differences in the 2021 and 2022 field experiments (Table S10). A highly significant regression ( $P<0.0001$ ,  $n=45$ ) was detected between the increases in %-glutenin and gluten strength scores that explained 85.3% of the variation (Table S13).

To separate the effects of the %-glutenins and the 7-CYS deletions on gluten strength, we calculated two independent regression lines using genotypes that either lack the  $\Delta gli$ -D2 deletion (wild type,  $\Delta gli$ -A2, and  $\Delta gli$ -B2) or that all have it ( $\Delta gli$ -D2 and  $\Delta gli$ -A2  $\Delta gli$ -D2, Fig. 7). Both regression lines showed similar slopes (Table S13), suggesting a similar relationship between %-glutenins and gluten strength. However, these lines were separated by a vertical gap (Fig. 7), which we interpreted as an additional positive effect of the  $\Delta gli$ -D2 deletion on gluten strength.

To test the significance of this difference, we integrated the normalized data from the two years (Table S13) and compared the lines with and without the  $\Delta gli$ -D2 deletion using the estimated %-glutenin content of each line as a covariate and the nine blocks from 2021 and 2022 as biological replicates. This analysis of covariance revealed a highly significant difference in gluten strength between genotypes with and without the  $\Delta gli$ -D2 deletion ( $P=0.0071$ , Table S13), which is separate from the effect of the differences in %-glutenin among genotypes.

Taken together, these results indicate that the large increases in gluten strength observed in the lines carrying the  $\Delta gli$ -D2 deletion are associated with the increases in %-glutenins caused by the deletion and a separate effect associated with the  $\Delta gli$ -D2 deletion. We hypothesize that this  $\Delta gli$ -D2 specific effect is the elimination of the detrimental 7-CYS gliadins that act as chain extension terminators limiting the size of the gluten macropolymer.

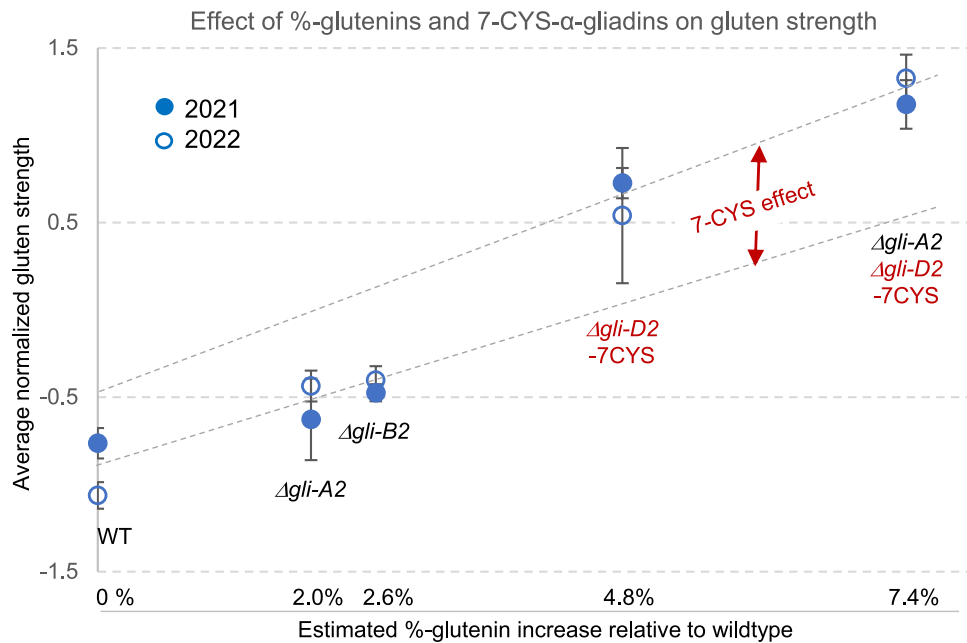


**Fig. 7** Effect of the increase in %-glutenins and deleted  $\alpha$ -gliadins with 7 cysteines (7-CYS) on gluten strength. Gluten strength was estimated from the average of six quality parameters associated to gluten strength (Table S13). Quality parameters for each of the two years (2021 filled circles and 2022 empty circles) were normalized by subtracting the trait mean and dividing by the standard deviation. Error bars are s.e.m. based on five biological replications in 2021

and four in 2022. Separate regressions were estimated for the lines with and without the  $\Delta gli-D2$  deletion to visualize the effects of the changes in %-glutenins independently of the differences in  $\alpha$ -gliadin with 7-CYS. Data and statistical analyses are in Table S13. This figure is based on multiple assumptions and should be interpreted as a preliminary representation of the two effects rather than as a precise quantification

## Discussion

### $\alpha$ -Gliadins show extensive variation in copy number and polymorphism levels

The  $\alpha$ -gliadins are present in wheat and closely related species of *Triticum* and *Aegilops*, but are not detected in rye or barley (Shewry and Tatham 1990), suggesting that they originated 3 to 5 million years ago (Gu et al. 2004). Comparisons of the  $\alpha$ -gliadins in each of the three loci across the different wheat sequenced genomes revealed frequent variation in copy number, as expected for a tandemly repeated multigene family. For example, the *GLI-A2* locus in Fielder (haplotype HA3) has eight complete annotated  $\alpha$ -gliadins, whereas 14 are annotated in the same locus in ArinaLrFor (HA1). By contrast, the *GLI-B2* locus in Fielder (HB7) includes 14 complete  $\alpha$ -gliadins, whereas only four are annotated in this locus in ArinaLrFor (HB4) (Table S5).

The *GLI-D2* locus showed reduced natural variation among the sequenced bread wheat genomes relative to the other two genomes (Tables S2–S4), which is consistent with the reduced variability of the *T. aestivum* D genome (Chao et al. 2007). We observed higher natural variation in *GLI-D2* among the *Ae. tauschii* sequenced genomes, and some of those polymorphisms were present in the exome captures of

several hexaploid wheats, including RIL143 (Table S4). This result suggests that these varieties may carry an *Ae. tauschii* introgression from the synthetic wheats developed at CIM-MYT (Rosyara et al. 2019) encompassing the *GLI-D2* locus.

Fortunately, the field evaluations of the UC-Central Red sister lines with and without the  $\Delta gli-D2$  introgression indicate that this putative introgression is not associated with negative effects on grain yield, kernel weight, test weight, or total grain protein content (Fig. 4). In summary, the haplotype analyses for the three *GLI2* loci presented in this study provide a useful framework to characterize the allelic diversity of the  $\alpha$ -gliadins from tetraploid and hexaploid wheat.

### *GLI-D2* includes $\alpha$ -gliadins with 7 cysteines that negatively affect gluten strength

An early sequencing study of wheat genomic clones including  $\alpha$ -gliadins from cultivar Cheyenne confirmed that most  $\alpha$ -gliadins encode proteins with six cysteines but also identified a few clones encoding  $\alpha$ -gliadins with seven cysteines (Anderson and Greene 1997). The authors of this study hypothesized that these unusual  $\alpha$ -gliadins might be incorporated into the glutenin fraction. Using two-dimensional electrophoretic separation (A-PAGE vs SDS-PAGE), Masci

et al. (2002) purified a glutenin fraction enriched in C-type low molecular weight glutenin subunits (LMW-GS) and mapped some of them to homeologous group 6. N-terminal amino acid sequencing revealed that 40% of the peptides from this fraction were similar to  $\alpha$ -gliadins (Masci et al. 2002). Due to the limited protein sequence obtained by this method, this study was not able to determine the number of cysteines present in the gliadins incorporated into the gluten polymer.

We took advantage of the multiple sequenced wheat genomes available today to re-explore this question. We confirmed that, indeed, there are two to three  $\alpha$ -gliadins encoding proteins with seven cysteines, and that these unusual gliadins are present exclusively in the D genome in all the examined bread wheat genomes. Moreover, we found 7-CYS  $\alpha$ -gliadins in the *Ae. tauschii* genomes, confirming that they were contributed to bread wheat by the diploid donor of the D genome (Table S5). The six cysteines found in the canonical  $\alpha$ -gliadins form three intra-molecular disulfide bonds (Müller and Wieser 1995), resulting in monomeric proteins with no cysteines available to form covalent bonds with the gluten polymer. It was previously hypothesized that 7-CYS  $\alpha$ -gliadins could form one intermolecular disulfide bond with the gluten polymer and act as terminators of the growing glutenin polymer chains, resulting in shorter gluten macropolymers (Kasarda et al. 1987; Masci et al. 2002; Shewry and Lafiandra 2022). Since the proportion of gluten macropolymer larger than 158 kDa is positively correlated with gluten strength (Gupta et al. 1993), the presence of 7-CYS  $\alpha$ -gliadins is predicted to be detrimental to gluten strength and breadmaking quality. Our proteomics studies demonstrated that, indeed, the 7-CYS  $\alpha$ -gliadins are preferentially enriched in the gluten macropolymer relative to the 6-CYS  $\alpha$ -gliadins (Table 2).

The effect of a *GLI-D2* deletion on gluten polymer size was previously determined in the cultivar Xiaoyan 81 (Li et al. 2018). This study found that the presence of the deletion was associated with a significant increase in the proportion of large glutenin macropolymers (> 250 kDa) and unextractable proteins (Li et al. 2018). We re-analyzed the published sequences of the  $\alpha$ -gliadins in wild-type Xiaoyan 81 (Li et al. 2018) and confirmed the presence of at least one  $\alpha$ -gliadin with seven cysteines in the D genome. We hypothesize that the deletion of this 7-CYS  $\alpha$ -gliadin may have contributed to the increased polymer size observed in the Xiaoyan 81 *GLI-D2* deletion.

The *GLI-D2* deletion in Xiaoyan 81 was also associated with significant increases in dough development and stability time and with increases in loaf volume relative to the control line (Li et al. 2018). The authors hypothesized that these favorable changes in the deletion line were the result of increases in the proportion of glutenins relative to gliadins, likely caused by compensatory higher expression of the

glutenin genes in the deletion line (Li et al. 2018). Although our  $\Delta$ *gli-D2* deletion also showed improved gluten strength, significant effects were not detected in  $\Delta$ *gli-A2* or  $\Delta$ *gli-B2* which also have deleted  $\alpha$ -gliadins (Fig. 5, Table S10).

The comparison of the prolamin proteomes of RIL143 and  $\Delta$ *gli-D2* provided an estimate of the proportion of  $\alpha$ -gliadins present in each of the three wheat genomes and the expected increases in %-glutenin in each deletion line. A highly significant regression between the %-glutenin increases and gluten strength (Table S13) confirmed the importance of glutenin content on this parameter. However, an analysis of covariance using the increase in %-glutenin as covariate confirmed the existence of a separate effect on gluten strength associated with the presence or absence of the  $\Delta$ *gli-D2* deletions (Fig. 7, Table S13). Taken together, these results indicate that both the increases in %-glutenins and a specific effect of  $\Delta$ *gli-D2* contributed to the large increases in gluten strength and improved breadmaking quality observed in the lines carrying the  $\Delta$ *gli-D2* deletion. We hypothesize that the  $\Delta$ *gli-D2* specific effect is associated with the elimination of the detrimental 7-CYS gliadins that act as chain extension terminators limiting the size of the gluten macropolymer.

## A path to reduced immunogenicity wheat

Although 30–40% of the human population express one or both CeD predisposing HLA-DQ allotypes HLA-DQ2 and HLA-DQ8, the prevalence of CeD is close to 1%. This difference indicates that additional genetic and environmental factors are involved in the onset of the disease (Abadie et al. 2024). Several studies suggest that one of those environmental factors is the level of exposure to immunogenic epitopes (Ivarsson et al. 2000; Koning 2012; Mearin et al. 1983; Megiorni et al. 2009). Therefore, a reduction in the level of wheat immunogenic epitopes may reduce the incidence of CeD at a population level. A logical start for this reduction path is the elimination of the immunodominant epitopes that result in high immune responses in the majority of the CeD patients. The elimination of immunogenic proteins with limited impact on breadmaking quality is an additional useful criterion to accelerate the deployment of loci with reduced immunogenic proteins.

The  $\alpha$ -gliadins are a desirable initial target since the *GLI2* loci segregate independently of the LMW-GS and HMW-GS, which have a major impact on gluten strength. In particular, the *GLI-D2* locus has on average 55.3% of the total epitopes and 81.2% of the immunodominant nanomers present in the  $\alpha$ -gliadins (Fig. 1, Table S5, average across Fielder, Chinese Spring, and ArinaLrFor). In addition, only the *GLI-D2* locus carries the highly immunogenic 17-mer (Anderson et al. 2000) and 33-mer peptides (Shan et al. 2002) formed by multiple overlapping immunodominant

nanomers. The presence of the 33-mer peptide only in the *GLI-D2* locus was also reported in the Italian variety Pegaso (Camerlengo et al. 2017).

In this study, we describe a  $\Delta gli\text{-}D2$  deletion that eliminates all the  $\alpha$ -gliadins from the *GLI-D2* locus and, therefore, all the highly immunogenic 17-mer and 33-mer epitopes and ~ 81% of the immunodominant nanomers present in the  $\alpha$ -gliadins. Although this deletion includes 259–267 genes in addition to the  $\alpha$ -gliadins, we observed no negative effects on grain yield, grain protein content, test weight, or kernel weight in the two genetic backgrounds evaluated over two years. Importantly, the  $\Delta gli\text{-}D2$  deletion showed a positive impact on gluten strength and breadmaking quality that was consistent in both low- and high-quality genetic backgrounds across the two years of replicated trials. A similar positive effect on gluten strength and breadmaking quality was observed in an independent  $\Delta gli\text{-}D2$  deletion in the Chinese bread wheat variety Xiaoyan 81 across four environments, which was also validated in a different genetic background with stronger HMW-GS alleles (Li et al. 2018). Increases in dough development time and stability measured by micro-mixograph tests were also observed in greenhouse experiments comparing Chinese Spring with lines carrying large terminal deletions of the short arm of chromosome 6DS. However, variable results were observed for other traits, likely associated with the large size of these deletions, which eliminated more than half of the short arms of chromosomes 6A, 6B, and 6D (van den Broeck et al. 2009).

Although immunogenic epitopes are present in the  $\alpha$ -gliadins from all three *GLI2* loci, the immunodominant epitopes are restricted to the *GLI-D2* and *GLI-A2* loci (Fig. 1, Table S5). Therefore, the simultaneous introgression of the  $\Delta gli\text{-}D2$  and  $\Delta gli\text{-}A2$  deletions can be used to further reduce the levels of immunodominant epitopes in hexaploid wheat. In this study, we show that the combination of these two deletions has no significant effects on grain yield (Fig. 4) and has the same beneficial effects on gluten strength and breadmaking quality as the single  $\Delta gli\text{-}D2$  deletion (Fig. 5). Different deletions for *GLI-A2* from cultivar 'Raeder' (Lafondra et al. 1987) and for *GLI-D2* from cultivar 'Saratovskaya 29' (Redaelli et al. 1994) were combined in the Italian bread wheat variety Pegaso, but the size of these deletions and their effect on breadmaking quality was not evaluated (Camerlengo et al. 2017).

We were not able to combine the  $\alpha$ -gliadin deletions in the three genomes because the two combinations including  $\Delta gli\text{-}B2$  showed abnormal flowers (Fig. S5) and were sterile. Wheat is a young polyploid species and often tolerates deletions of one and sometimes two homeologs, but deletions of three homeologs are expected to have the same effects as in a diploid species (Uauy et al. 2017). The risk of deleting essential or important non-gliadin genes in all three homeologs limits the use of large deletions to obtain triple null

mutants for the  $\alpha$ -gliadins. Smaller  $\alpha$ -gliadin deletions or CRISPR editing of the  $\alpha$ -gliadins in at least one of the three genomes will be likely required to generate simultaneous deletions of all  $\alpha$ -gliadins and study their effect on quality and agronomic performance.

Although the combined  $\Delta gli\text{-}A2$   $\Delta gli\text{-}D2$  deletions would eliminate the known immunodominant epitopes present in the  $\alpha$ -gliadins, there are additional immunodominant epitopes (DQ2.5-glia- $\omega 1$  and DQ2.5-glia- $\omega 2$ ) in the  $\omega$ -gliadins in the *GLI-A1*, *GLI-B1*, and *GLI-D1* loci. Most of these immunodominant epitopes are present in the *GLI-D1* locus. Fortunately, there is a published 1D deletion originally identified in the French cultivar 'Darius' and then transferred to the cultivar 'Pegaso' (Camerlengo et al. 2017) that eliminates all the  $\omega$ - and  $\gamma$ -gliadins. However, most of the linked LMW-GS are not deleted (Branlard et al. 2003). We are currently combining this deletion with  $\Delta gli\text{-}A2$  and  $\Delta gli\text{-}D2$  and evaluating its effect on grain yield and quality. There are other CRISPR-induced deletions and knockouts including multiple gliadin loci but not all of them are publicly available (Jouanin et al. 2019; Sánchez-León et al. 2018).

Another useful resource is a CRISPR line in the cultivar Fielder that eliminated all the  $\omega$ -gliadins and some  $\gamma$ -gliadins (Yu et al. 2024). These deletions were associated with a significant increase in the ratio of glutenins to gliadins, the ratio of polymeric to monomeric proteins, and the proportion of gluten macropolymer in total protein. These changes were associated with significant increases in mixograph peak time and farinograph stability time, two parameters associated with improved gluten strength (Yu et al. 2024). These results, together with the effects of the  $\alpha$ -gliadin deletions reported in this study, indicate that a large proportion of the immunogenic  $\alpha$ -,  $\omega$ -, and  $\gamma$ -gliadins can be eliminated without negatively affecting breadmaking quality and, in some cases, even generating positive effects in gluten strength and other breadmaking quality parameters.

Even if all the immunodominant epitopes are eliminated, the resulting plants will not be safe for people that already have CeD because of the presence of residual epitopes. The elimination of all epitopes will require the modification of LMW-GS and HMW-GS that are essential for gluten polymer formation and that will likely need to be replaced with transgenic functional versions without the epitopes to restore the lost breadmaking quality. Although the development of CeD-safe wheats will likely have to wait for a broader acceptance of transgenic technologies, the development of wheats lines with reduced immunogenicity is an achievable intermediate objective.

The development of wheat lines without immunodominant epitopes will be useful to quantify the impact of this reduction on the onset of the CeD disease in genetically predisposed individuals and the incidence of CeD at the

population level. Meanwhile, the  $\Delta gli\text{-}A2$  and  $\Delta gli\text{-}D2$  lines developed in this study can be combined to eliminate the immunodominant epitopes from the  $\alpha$ -gliadins. In particular, the incorporation of the  $\Delta gli\text{-}D2$  deletion into commercial bread wheat varieties will simultaneously eliminate many immunodominant epitopes and improve gluten strength and breadmaking quality. To accelerate the deployment of these deletions in wheat breeding programs, we have deposited the RIL143  $\Delta gli\text{-}A2$  (PI 704906),  $\Delta gli\text{-}B2$  (PI 704907), and  $\Delta gli\text{-}D2$  (PI 704908) deletions in GRIN-Global and made them publicly available without any restrictions.

**Supplementary Information** The online version contains supplementary material available at <https://doi.org/10.1007/s00122-025-04882-3>.

**Acknowledgements** We thank Huiqiong Lin (UC Davis) for her help with the floret pictures of the Kronos wild type and the combined deletion lines.

**Author contribution statement** MGR contributed to writing—original draft, data curation, investigation, visualization, statistical analyses, and formal analysis. WZ was involved in investigation, methodology, writing, reviewing, and editing. XZ contributed to methodology. JZ was involved in formal analysis, writing, reviewing, and editing. GG contributed to data curation, methodology, writing—reviewing, and editing. GB was involved in data curation, bioinformatics methodology, reviewing, and editing. JH contributed to field methodology, data curation, reviewing, and editing. TV and CC were involved in quality methodology, supervision, resources, reviewing, and editing. SF contributed to quality experiments, data curation, and writing. JD was involved in conceptualization, visualization, statistical analyses, funding acquisition, project administration, supervising, formal analysis, and writing—reviewing and editing.

**Funding** This project was supported by the Celiac Disease Foundation, the Agriculture and Food Research Initiative Competitive Grant 2022-68013-36439 (WheatCAP) from the USDA National Institute of Food and Agriculture and by the Howard Hughes Medical Institute. JD and MGR acknowledge support from the Foundation for Food and Agriculture Research.

**Data availability** Raw data and statistical analysis are included in the Supplementary Data. The  $\alpha$ -gliadin deletion lines in the hexaploid wheat breeding line RIL143 were deposited in GRIN-Global under the germplasm identification numbers PI 704906 ( $\Delta gli\text{-}A2$ ), PI 704907 ( $\Delta gli\text{-}B2$ ), and PI 704908 ( $\Delta gli\text{-}D2$ ).

## Declarations

**Conflict of interest** The authors declare that they have no conflict of interest.

**Open Access** This article is licensed under a Creative Commons Attribution 4.0 International License, which permits use, sharing, adaptation, distribution and reproduction in any medium or format, as long as you give appropriate credit to the original author(s) and the source, provide a link to the Creative Commons licence, and indicate if changes were made. The images or other third party material in this article are included in the article's Creative Commons licence, unless indicated otherwise in a credit line to the material. If material is not included in the article's Creative Commons licence and your intended use is not permitted by statutory regulation or exceeds the permitted use, you will

need to obtain permission directly from the copyright holder. To view a copy of this licence, visit <http://creativecommons.org/licenses/by/4.0/>.

## References

Abadie V, Han AS, Jabri B, Sollid LM (2024) New insights on genes, gluten, and immunopathogenesis of celiac disease. *Gastroenterology* 167:4–22. <https://doi.org/10.1053/j.gastro.2024.03.042>

Anderson OD, Greene FC (1997) The alpha-gliadin gene family.2. DNA and protein sequence variation, subfamily structure, and origins of pseudogenes. *Theor Appl Genet* 95:59–65. <https://doi.org/10.1007/s001220050532>

Anderson RP, Degano P, Godkin AJ, Jewell DP, Hill AVS (2000) In vivo antigen challenge in celiac disease identifies a single transglutaminase-modified peptide as the dominant A-gliadin T-cell epitope. *Nat Med* 6:337–342. <https://doi.org/10.1038/73200>

Athiyannan N, Abrouk M, Boshoff WHP, Cauet S, Rodde N, Kudrna D, Mohammed N, Bettgenhaeuser J, Botha KS, Derman SS, Wing R, Prins R, Krattinger SG (2022) Long-read genome sequencing of bread wheat facilitates disease resistance gene cloning. *Nat Genet* 54:227–231. <https://doi.org/10.1038/s41588-022-01022-1>

Avni R, Nave M, Barad O, Baruch K, Twardziok SO, Gundlach H, Hale I, Mascher M, Spannagl M, Wiebe K, Jordan KW, Golan G, Deek J, Ben-Zvi B, Ben-Zvi G, Himmelbach A, MacLachlan RP, Sharpe AG, Fritz A, Ben-David R, Budak H, Fahima T, Korol A, Faris JD, Hernandez A, Mikel MA, Levy AA, Steffenson B, Maccaferri M, Tuberosa R, Cattivelli L, Faccioli P, Ceriotti A, Kashkush K, Pourkheirandish M, Komatsuda T, Eilam T, Sela H, Sharon A, Ohad N, Chamovitz DA, Mayer KFX, Stein N, Ronen G, Peleg Z, Pozniak CJ, Akhunov ED, Distelfeld A (2017) Wild emmer genome architecture and diversity elucidate wheat evolution and domestication. *Science* 357:93–97. <https://doi.org/10.1126/science.aan0032>

Blake VC, Birkett C, Matthews DE, Hane DL, Bradbury P, Jannink JL (2012) The Triticeae Toolbox: combining phenotype and genotype data to advance small-grains breeding. *Plant Genome*. <https://doi.org/10.3835/plantgenome2014.12.0099>

Bradauskienė V, Vaiciulyte-Funk L, Martinaitiene D, Andruskiene J, Verma AK, Lima JPM, Serin Y, Catassi C (2023) Wheat consumption and prevalence of celiac disease: correlation from a multilevel analysis. *Crit Rev Food Sci* 63:18–32. <https://doi.org/10.1080/10408398.2021.1939650>

Branlard G, Dardevet M, Amiour N, Igrejas G (2003) Allelic diversity of HMW and LMW glutenin subunits and omega-gliadins in French bread wheat (*Triticum aestivum* L.). *Genet Resour Crop Evol* 50:669–679. <https://doi.org/10.1023/A:1025077005401>

Camerlengo F, Sestili F, Silvestri M, Colaprico G, Margiotta B, Ruggeri R, Lupi R, Masci S, Lafiandra D (2017) Production and molecular characterization of bread wheat lines with reduced amount of alpha-type gliadins. *BMC Plant Biol* 17:248. <https://doi.org/10.1186/s12870-017-1211-3>

Chao SM, Zhang WJ, Dubcovsky J, Sorrells M (2007) Evaluation of genetic diversity and genome-wide linkage disequilibrium among US wheat (*Triticum aestivum* L.) germplasm representing different market classes. *Crop Sci* 47:1018–1030. <https://doi.org/10.2135/cropsci2006.06.0434>

Chen S, Hegarty J, Shen T, Hua L, Li H, Luo J, Li H, Bai S, Zhang C, Dubcovsky J (2021) Stripe rust resistance gene *Yr34* (synonym *Yr48*) is located within a distal translocation of *Triticum monococcum* chromosome 5A<sup>m</sup>L into common wheat. *Theor Appl Genet* 134:2197–2211. <https://doi.org/10.1007/s00122-021-03816-z>

Chlubnova M, Christophersen AO, Sandve GKF, Lundin KEA, Jahnsen J, Dahal-Koirala S, Sollid LM (2023) Identification of gluten T cell epitopes driving celiac disease. *Sci Adv* 9:eade5800. <https://doi.org/10.1126/sciadv.ade5800>

Gu YQ, Crossman C, Kong X, Luo MC, You FM, Coleman-Derr D, Dubcovsky J, Anderson OD (2004) Genomic organization of the complex  $\alpha$ -gliadin gene loci in wheat. *Theor Appl Genet* 109:648–657. <https://doi.org/10.1007/s00122-004-1672-2>

Gupta RB, Khan K, Macritchie F (1993) Biochemical basis of flour properties in bread wheats. I. Effects of variation in the quantity and size distribution of polymeric protein. *J Cereal Sci* 18:23–41. <https://doi.org/10.1006/jcres.1993.1031>

Ivarsson A, Persson LÅ, Nyström I, Ascher H, Cavell B, Danielsson L, Dannaeus A, Lindberg T, Lindquist B, Stenhammar L, Hernell O (2000) Epidemic of coeliac disease in Swedish children. *Acta Paediatr* 89:165–171. <https://doi.org/10.1080/080352500750028771>

Jabri B, Sollid LM (2017) T cells in celiac disease. *J Immunol* 198:3005–3014. <https://doi.org/10.4049/jimmunol.1601693>

Jouanin A, Schaart JG, Boyd LA, Cockram J, Leigh FJ, Bates R, Wallington EJ, Visser RGF, Smulders MJM (2019) Outlook for coeliac disease patients: towards bread wheat with hypoimmunogenic gluten by gene editing of  $\alpha$ - and  $\gamma$ -gliadin gene families. *BMC Plant Biol* 19:333. <https://doi.org/10.1186/s12870-019-1889-5>

Juhász A, Belova T, Florides CG, Maulis C, Fischer I, Gell G, Birinyi Z, Ong J, Keeble-Gagnere G, Maharajan A, Ma W, Gibson P, Jia J, Lang D, Mayer KFX, Spannagl M, Tye-Din JA, Appels R, Olsen OA, International Wheat Genome Sequencing C (2018) Genome mapping of seed-borne allergens and immunoresponsive proteins in wheat. *Sci Adv* 4:eaar8602. <https://doi.org/10.1126/sciadv.aar8602>

Kale SM, Schulthess AW, Padmarasu S, Boeven PHG, Schacht J, Himmelbach A, Steuernagel B, Wulff BBH, Reif JC, Stein N, Mascher M (2022) A catalogue of resistance gene homologs and a chromosome-scale reference sequence support resistance gene mapping in winter wheat. *Plant Biotechnol J* 20:1730–1742. <https://doi.org/10.1111/pbi.13843>

Kasarda DD, Adalsteins AE, Laird NF (1987) Gamma-gliadins with alpha-type structure coded on chromosome 6B of the wheat (*Triticum aestivum* L.) cultivar Chinese Spring. In: Proceedings of the 3rd international workshop of gluten proteins, Budapest, Hungary, pp 20–29

King JA, Jeong J, Underwood FE, Quan JS, Panaccione N, Windsor JW, Coward S, deBruyn J, Ronksley PE, Shaheen AA, Quan HD, Godley J, van Zanten SV, Lebwohl B, Ng SC, Ludvigsson JF, Kaplan GG (2020) Incidence of Celiac Disease is increasing over time: a systematic review and meta-analysis. *Am J Gastroenterol* 115:507–525. <https://doi.org/10.14309/ajg.0000000000000523>

Koning F (2012) Celiac disease: quantity matters. *Semin Immunopathol* 34:541–549. <https://doi.org/10.1007/s00281-012-0321-0>

Krasileva KV, Vasquez-Gross HA, Howell T, Bailey P, Paraiso F, Clissold L, Simmonds J, Ramirez-Gonzalez RH, Wang X, Borrill P, Fosker C, Ayling S, Phillips AL, Uauy C, Dubcovsky J (2017) Uncovering hidden variation in polyploid wheat. *Proc Natl Acad Sci USA* 114:E913–E921. <https://doi.org/10.1073/pnas.1619268114>

Lafiandra D, Colaprico G, Kasarda DD, Porceddu E (1987) Null alleles for gliadin blocks in bread and durum-wheat cultivars. *Theor Appl Genet* 74:610–616. <https://doi.org/10.1007/BF00288860>

Li D, Jin HB, Zhang KP, Wang ZJ, Wang FM, Zhao Y, Huo NX, Liu X, Gu YQ, Wang DW, Dong LL (2018) Analysis of the *Gli-D2* locus identifies a genetic target for simultaneously improving the breadmaking and health-related traits of common wheat. *Plant J* 95:414–426. <https://doi.org/10.1111/tpj.13956>

Li H (2013) Aligning sequence reads, clone sequences and assembly contigs with BWA-MEM. *arXiv preprint arXiv:1303.3997*

Lowe I, Jankuloski L, Chao S, Chen X, See D, Dubcovsky J (2011) Mapping and validation of QTL which confer partial resistance to broadly virulent post-2000 North American races of stripe rust in hexaploid wheat. *Theor Appl Genet* 123:143–157. <https://doi.org/10.1007/s00122-011-1573-0>

Luo MC, Gu YQ, Puiu D, Wang H, Twardziok SO, Deal KR, Huo NX, Zhu TT, Wang L, Wang Y, McGuire PE, Liu SY, Long H, Ramasamy RK, Rodriguez JC, Van SL, Yuan LX, Wang ZZ, Xia ZQ, Xiao LC, Anderson OD, Ouyang SH, Liang Y, Zimin AV, Pertea G, Qi P, Ennenet JLB, Dai XT, Dawson MW, Müller HG, Kugler K, Rivarola-Duarte L, Spannagl M, Mayer KFX, Lu FH, Bevan MW, Leroy P, Li PC, You FM, Sun QX, Liu ZY, Lyons E, Wicker T, Salzberg SL, Devos KM, Dvorák J (2017) Genome sequence of the progenitor of the wheat D genome *Aegilops tauschii*. *Nature* 551:498–502. <https://doi.org/10.1038/nature24486>

Maccaferri M, Harris NS, Twardziok SO, Pasam RK, Gundlach H, Spannagl M, Ormanbekova D, Lux T, Prade VM, Milner SG, Himmelbach A, Mascher M, Bagnaresi P, Faccioli P, Cozzi P, Lauria M, Lazzari B, Stella A, Manconi A, Gnocchi M, Moscatelli M, Avni R, Deek J, Biyiklioglu S, Frascaroli E, Cornetti S, Salvi S, Sonnante G, Desiderio F, Mare C, Crosatti C, Mica E, Ozkan H, Kilian B, De Vita P, Marone D, Joukhadar R, Mazzucotelli E, Nigro D, Gadaleta A, Chao SM, Faris JD, Melo ATO, Pumphrey M, Pecchioni N, Milanesi L, Wiebe K, Ens J, MacLachlan RP, Clarke JM, Sharpe AG, Koh CS, Liang KYH, Taylor GJ, Knox R, Budak H, Mastrangelo AM, Xu SS, Stein N, Hale I, Distelfeld A, Hayden MJ, Tuberosa R, Walkowiak S, Mayer KFX, Ceriotti A, Pozniak CJ, Cattivelli L (2019) Durum wheat genome highlights past domestication signatures and future improvement targets. *Nat Genet* 51:885–895. <https://doi.org/10.1038/s41588-019-0381-3>

Masci S, Rovelli L, Kasarda DD, Vensel WH, Lafiandra D (2002) Characterisation and chromosomal localisation of C-type low-molecular-weight gliadin subunits in the bread wheat cultivar Chinese Spring. *Theor Appl Genet* 104:422–428. <https://doi.org/10.1007/s0012200100761>

Mearin ML, Biemond I, Pena AS, Polanco I, Vazquez C, Schreuder GT, de Vries RR, van Rood JJ (1983) HLA-DR phenotypes in Spanish coeliac children: their contribution to the understanding of the genetics of the disease. *Gut* 24:532–537. <https://doi.org/10.1136/gut.24.6.532>

Megiorni F, Mora B, Bonamico M, Barbato M, Nenna R, Maiella G, Lulli P, Mazzilli MC (2009) HLA-DQ and risk gradient for celiac disease. *Hum Immunol* 70:55–59. <https://doi.org/10.1016/j.humimm.2008.10.018>

Müller S, Wieser H (1995) The location of disulfide bonds in alpha-type gliadins. *J Cereal Sci* 22:21–27. [https://doi.org/10.1016/S0733-5210\(05\)80004-9](https://doi.org/10.1016/S0733-5210(05)80004-9)

R-Core-Team (2021) R: a language and environment for statistical computing. R Foundation for Statistical Computing, Vienna

Redaelli R, Metakovsky EV, Davidov SD, Pogna NE (1994) Two-dimensional mapping of gliadins using biotypes and null mutants of common wheat cultivar Saratovskaya-29. *Hereditas* 121:131–137. <https://doi.org/10.1111/j.1601-5223.1994.00131.x>

Rosyara U, Kishii M, Payne T, Sansaloni CP, Singh RP, Braun HJ, Dreisigacker S (2019) Genetic contribution of synthetic hexaploid wheat to CIMMYT's spring bread wheat breeding germplasm. *Sci Rep* 9:12355. <https://doi.org/10.1038/s41598-019-47936-5>

Sánchez B, Barro F, Smulders MJM, Gilissen LJWJ, Rodríguez-Cerezo E (2023) Socioeconomic impact of low-gluten, celiac-safe wheat developed through gene editing. *Publications Office of the European Union*, Luxembourg. <https://doi.org/10.2760/280847>

Sánchez-León S, Gil-Humanes J, Ozuna CV, Giménez MJ, Sousa C, Voytas DF, Barro F (2018) Low-gluten, nontransgenic wheat

engineered with CRISPR/Cas9. *Plant Biotechnol J* 16:902–910. <https://doi.org/10.1111/pbi.12837>

Sato K, Abe F, Mascher M, Haberer G, Gundlach H, Spannagl M, Shirasawa K, Isobe S (2021) Chromosome-scale genome assembly of the transformation-amenable common wheat cultivar “Fielder.” *DNA Res* 28:dsab008. <https://doi.org/10.1093/dnares/dsab008>

Shan L, Molberg Ø, Parrot I, Hausch F, Filiz F, Gray GM, Sollid LM, Khosla C (2002) Structural basis for gluten intolerance in Celiac sprue. *Science* 297:2275–2279. <https://doi.org/10.1126/science.1074129>

Shewry PR, Lafiandra D (2022) Wheat glutenin polymers 1. Structure, assembly and properties. *J Cereal Sci* 106:103486. <https://doi.org/10.1016/j.jcs.2022.103486>

Shewry PR, Tatham AS (1990) The prolamin storage proteins of cereal seeds—structure and evolution. *Biochem J* 267:1–12. <https://doi.org/10.1042/bj2670001>

Singh NK, Shepherd KW, Cornish GB (1991) A simplified SDS-PAGE procedure for separating LMW subunits of glutenin. *J Cereal Sci* 14:203–208. [https://doi.org/10.1016/S0733-5210\(09\)80039-8](https://doi.org/10.1016/S0733-5210(09)80039-8)

Sollid LM, Qiao SW, Anderson RP, Gianfrani C, Koning F (2012) Nomenclature and listing of celiac disease relevant gluten T-cell epitopes restricted by HLA-DQ molecules. *Immunogenetics* 64:455–460. <https://doi.org/10.1007/s00251-012-0599-z>

Sollid LM, Tye-Din JA, Qiao SW, Anderson RP, Gianfrani C, Koning F (2020) Update 2020: nomenclature and listing of celiac disease-relevant gluten epitopes recognized by CD4<sup>+</sup> T cells. *Immunogenetics* 72:85–88. <https://doi.org/10.1007/s00251-019-01141-w>

Tye-Din JA, Stewart JA, Dromey JA, Beissbarth T, van Heel DA, Tatham A, Henderson K, Mannering SI, Gianfrani C, Jewell DP, Hill AV, McCluskey J, Rossjohn J, Anderson RP (2010) Comprehensive, quantitative mapping of T cell epitopes in gluten in celiac disease. *Sci Transl Med* 2:41–51. <https://doi.org/10.1126/scitranslmed.3001012>

Uauy C, Wulff BBH, Dubcovsky J (2017) Combining traditional mutagenesis with new high-throughput sequencing and genome editing to reveal hidden variation in polyploid wheat. *Annu Rev Genet* 51:435–454. <https://doi.org/10.1146/annurev-genet-120116-024533>

Vader W, Kooy Y, Van Veelen P, De Ru A, Harris D, Benckhuijsen W, Peña S, Mearin L, Drijfhout JW, Koning F (2002) The gluten response in children with celiac disease is directed toward multiple gliadin and glutenin peptides. *Gastroenterology* 122:1729–1737. <https://doi.org/10.1053/gast.2002.33606>

van den Broeck HC, van Herpen TWJM, Schuit C, Salentijn EMJ, Dekking L, Bosch D, Hamer RJ, Smulders MJM, Gilissen LJWJ, van der Meer IM (2009) Removing celiac disease-related gluten proteins from bread wheat while retaining technological properties: a study with Chinese Spring deletion lines. *BMC Plant Biol* 9:41. <https://doi.org/10.1186/1471-2229-9-41>

Walkowiak S, Gao LL, Monat C, Haberer G, Kassa MT, Brinton J, Ramirez-Gonzalez RH, Kolodziej MC, Delorean E, Thambugala D, Klymiuk V, Byrns B, Gundlach H, Bandi V, Siri JN, Nilsen K, Aquino C, Himmelbach A, Copetti D, Ban T, Venturini L, Bevan M, Clavijo B, Koo DH, Ens J, Wiebe K, N'Diaye A, Fritz AK, Gutwin C, Fiebig A, Fosker C, Fu BX, Accinelli GG, Gardner KA, Fradgley N, Gutierrez-Gonzalez J, Halstead-Nussloch G, Hatakeyama M, Koh CS, Deek J, Costamagna AC, Fobert P, Heavens D, Kanamori H, Kawaura K, Kobayashi F, Krasileva K, Kuo T, McKenzie N, Murata K, Nabeka Y, Paape T, Padmarasu S, Percival-Alwyn L, Kagale S, Scholz U, Sese J, Juliana P, Singh R, Shimizu-Inatsugi R, Swarbreck D, Cockram J, Budak H, Tameshige T, Tanaka T, Tsuji H, Wright J, Wu JZ, Steuernagel B, Small I, Cloutier S, Keeble-Gagnere G, Muehlbauer G, Tibbets J, Nasuda S, Melonek J, Hucl PJ, Sharpe AG, Clark M, Legg E, Bharti A, Langridge P, Hall A, Uauy C, Mascher M, Krattinger SG, Handa H, Shimizu KK, Distelfeld A, Chalmers K, Keller B, Mayer KFX, Poland J, Stein N, McCartney CA, Spannagl M, Wicker T, Pozniak CJ (2020) Multiple wheat genomes reveal global variation in modern breeding. *Nature* 588:277–283. <https://doi.org/10.1038/s41586-020-2961-x>

Wang DW, Li D, Wang J, Zhao Y, Wang Z, Yue GD, Liu X, Qin H, Zhang K, Dong L, Wang D (2017) Genome-wide analysis of complex wheat gliadins, the dominant carriers of celiac disease epitopes. *Sci Rep-Uk* 7:44609. <https://doi.org/10.1038/srep44609>

Wieser H, Koehler P, Scherf KA (2022) Chemistry of wheat gluten proteins: quantitative composition. *Cereal Chem* 100:36–55. <https://doi.org/10.1002/cche.10553>

Yu Z, Yunusbaev U, Fritz A, Tilley M, Akhunova A, Trick H, Akhunov E (2024) CRISPR-based editing of the  $\omega$ - and  $\gamma$ -gliadin gene clusters reduces wheat immunoreactivity without affecting grain protein quality. *Plant Biotechnol J* 22:892–903. <https://doi.org/10.1111/pbi.14231>

Zhou Y, Bai SL, Li H, Sun GL, Zhang DL, Ma FF, Zhao XP, Nie F, Li JY, Chen LY, Lv LL, Zhu LL, Fan RX, Ge YF, Shaheen A, Guo GH, Zhang Z, Ma JC, Liang HH, Qiu XL, Hu JM, Sun T, Hou JY, Xu HX, Xue SL, Jiang WK, Huang JL, Li SP, Zou CS, Song CP (2021) Introgressing the *Aegilops tauschii* genome into wheat as a basis for cereal improvement. *Nat Plants* 7:774–786. <https://doi.org/10.1038/s41477-021-00934-w>

Zhu TT, Wang L, Rodriguez JC, Deal KR, Avni R, Distelfeld A, McGuire PE, Dvorak J, Luo MC (2019) Improved genome sequence of wild emmer wheat Zavitan with the aid of optical maps. *G3-Genes Genom Genet* 9:619–624. <https://doi.org/10.1534/g3.118.200902>

**Publisher's Note** Springer Nature remains neutral with regard to jurisdictional claims in published maps and institutional affiliations.